# Oxidative reactions catalyzed by hydrogen peroxide produced by *Streptococcus pneumoniae* and other Streptococci Cause the Release and Degradation of Heme from Hemoglobin

**Babek Alibayov[1], Anna Scasny[1], Faidad Khan[1], Aidan Creel[1,2], Perriann Smith[1,3], Ana G. Jop Vidal[1], Fa'alataitaua M. Fitisemanu[4], Teresita Padilla-Benavides[4], Jeffrey Weiser[5], and Jorge E. Vidal[1,#],**

[1]Department of Cell and Molecular Biology, School of Medicine, and [2]Summer Undergraduate Research Experience Program (SURE), School of Graduate Studies in the Health Sciences, University of Mississippi Medical Center, Jackson MS; [3]Mississippi INBRE Research Scholar, University of Southern Mississippi, Hattiesburg MS; [4]Department of Molecular Biology and Biochemistry, Wesleyan University, Middletown CT; [5]Department of Microbiology, NYU Langone Health, New York NY,

Running title: Spn-$H_2O_2$ oxidizes hemoglobin degrading heme

[#]Address correspondence to:

Jorge E. Vidal, PhD

2500 North State Street, Jackson Mississippi 39216

Phone: (601) 984-1711, Fax: (601) 984-1501

Email: jvidal@umc.edu

**Abstract**

*Streptococcus pneumoniae* (Spn) strains cause pneumonia that kills millions every year worldwide. Spn produces Ply, a hemolysin that lyses erythrocytes releasing hemoglobin and also produces the pro-oxidant hydrogen peroxide (Spn-$H_2O_2$) during growth. The hallmark of the pathophysiology of hemolytic diseases is the oxidation of hemoglobin but oxidative reactions catalyzed by Spn-$H_2O_2$ has been poorly studied. We characterized the oxidation of hemoglobin by Spn-$H_2O_2$. We prepared a series of single (Δ*spxB*, or Δ*lctO*), double mutant (Δ*spxB*Δ*lctO*) and complemented strains in TIGR4, D39 and EF3030. We then utilized an *in vitro* model with oxy-hemoglobin to demonstrate that oxy-hemoglobin was oxidized rapidly, within 30 min of incubation, by Spn-$H_2O_2$ to met-hemoglobin and that the main source of Spn-$H_2O_2$ was pyruvate oxidase (SpxB). Moreover, extended incubation caused the release and the degradation of heme. We then assessed oxidation of hemoglobin and heme degradation by other bacteria inhabitants of the respiratory tract. All hydrogen peroxide-producing streptococci tested caused the oxidation of hemoglobin and heme degradation whereas those bacterial species that produce <1 μM $H_2O_2$, neither oxidized hemoglobin nor degraded heme. An *ex vivo* bacteremia model confirmed that oxidation of hemoglobin and heme degradation occurred concurrently with hemoglobin that was released from erythrocytes by Ply. Finally, gene expression studies demonstrated that heme, but not red blood cells or hemoglobin induced an upregulated transcription of the *spxB* gene. Oxidation of hemoglobin may be important for pathogenesis and for the symbiosis of hydrogen peroxide-producing bacteria with other species by providing nutrients such as iron.

46 **Introduction.**

47 *Streptococcus pneumoniae* (Spn) colonizes the lower respiratory epithelium, causing
48 pneumonia that can progress to invasive pneumococcal disease (IPD)(1-4). Spn mainly affects the
49 most vulnerable populations: young children, immunocompromised patients, and the elderly (1, 4,
50 5). Globally, Spn causes ~15 million cases of illness each year, leading to more than a million deaths
51 due to pneumonia (6-8). Pneumonia is an acute infection of the pulmonary parenchyma that
52 presents with pulmonary hemorrhage, inflammatory congestion, hepatization, suppurative
53 infiltration and lung parenchymal injury (4, 9-13). If left untreated, Spn invades the bloodstream,
54 producing septic shock, multiorgan failure, cardiotoxicity, and death within days from onset (4, 9-12,
55 14, 15).

56 Spn strains produce the toxin pneumolysin (Ply) that has cytotoxic activity against lung
57 epithelial and endothelial cells (16-18). Ply is a 53-kDa surface located protein (19, 20) that can also
58 be released through autolysis (21, 22). Besides its toxicity against cells, Ply has hemolytic activity
59 against erythrocytes of several mammalian species and hemolysis is observed whether Ply is
60 released into the supernatant or located on the bacterial membrane (20). Under standard culture
61 conditions, i.e., growing bacteria at 37°C in a 5% $CO_2$ atmosphere, Ply is responsible for almost all
62 hemolytic activity in cultures of Spn strains (11), causing the release of a large amount of
63 hemoglobin into the supernatant (20, 21, 23). Transcription of the *ply* gene encoding this
64 pneumolysin is upregulated when Spn is cultured under conditions mimicking lung infection (24)
65 and therefore, Ply-induced release of hemoglobin is expected to occur during pneumococcal lung
66 infection.

67 Hemoglobin is a tetrameric protein (64 kDa) made of four subunits, two alpha and two beta
68 chains. Each subunit contains a heme center that reversibly binds oxygen through a penta-

69 coordinate heme molecule containing ferrous iron ($Fe^{+2}$), known as oxy-hemoglobin (25, 26). When
70 hemoglobin is released from erythrocytes, heme-hemoglobin can be observed by spectroscopy at
71 ~415 nm (25, 27, 28). This region is known as the Soret region peak and represents heme-
72 hemoglobin, while the alpha and beta chains are characterized by two absorption peaks of ~540
73 and ~570 nm (27, 28). Cell-free heme is toxic to cells because of its potential to generate toxic
74 radicals (29).

75 Release of hemoglobin during hemolytic disease such as sickle cell disease and other
76 hemorrhagic conditions, causes oxidation of hemoglobin (30). Oxidized hemoglobin releases heme,
77 which in turn induces adverse effects including leukocyte activation, cytokine up-regulation, and
78 production of oxidants leading to lung epithelial injury and damage to the vascular system (29-31).
79 Reactive oxygen species (ROS), such as nitric oxide (NO) (32) hypochlorous acid conjugate base
80 (OCl-)(24), and $H_2O_2$ (33, 34), drive a catalytic cycle including the oxidation of oxy-hemoglobin to
81 ferryl hemoglobin (Hb-$Fe^{+4}$), and auto - reduction of the ferryl intermediate to met-hemoglobin (Hb-
82 $Fe^{+3}$) that is detected by spectroscopy at 405 nm (35, 36). Additional pro-oxidant molecules, such as
83 $H_2O_2$, produce more ferryl hemoglobin and cause heme degradation (28, 36). Thus, the oxidation of
84 hemoglobin results in highly oxidizing ferryl hemoglobin (Hb-$Fe^{4+}$), met-hemoglobin (Hb-$Fe^{3+}$) and
85 the release of toxic heme that disrupts the mitochondria membrane potential of lung epithelial cells
86 and endothelial cells, and caused lipid peroxidation (28, 30, 36-38).

87 Because Spn causes hemorrhage in the lung and produces a large amount of highly reactive
88 $H_2O_2$ (39, 40), oxidation of cell-free hemoglobin might occur during pneumococcal disease. $H_2O_2$ is a
89 by-product of the oxidation of pyruvate, end product of the glycolysis, produced by the enzyme
90 pyruvate oxidase (SpxB) (41, 42). This reaction consumes oxygen and produces $H_2O_2$. In the absence
91 of oxygen, pyruvate is converted to L-lactate while in the presence of molecular $O_2$, L-lactate feeds

92 back to pyruvate, via lactate oxidase (LctO), in a reaction that also produces $H_2O_2$ (41, 42). It has
93 been calculated that ~85% of $H_2O_2$ released in cultures of Spn occurs through the reaction catalyzed
94 by SpxB, whereas the remaining ~15% is attributed to LctO (43, 44). Experiments using animal
95 models have demonstrated that Spn-$H_2O_2$ plays a role in lung colonization, and in the translocation
96 of Spn from the lungs to the bloodstream (45-48). Details of the mechanism(s) are largely unknown.
97 We recently discovered that Spn-$H_2O_2$ oxidizes hemoglobin to met-hemoglobin, a non-oxygen
98 binding form of hemoglobin (23). We also demonstrated that the oxidation of hemoglobin causes
99 the characteristic greenish halo around pneumococcal colonies grown on blood agar plates, known
100 as alpha hemolysis (23). Thus, the phenotype known as alpha hemolysis is not hemolysis but the
101 oxidation of hemoglobin to met-hemoglobin (23). Another alpha-hemolytic streptococci, *S. gordonii*,
102 oxidizes hemoglobin to met-hemoglobin through catalytic reactions driven by $H_2O_2$ (49).
103 Oxidation of cell-free hemoglobin induces lung injury in patients with acute respiratory distress
104 syndrome (31), and in children with SCD, oxidation of hemoglobin (Hb)S to Hb-$Fe^{4+}$ and then its
105 reduction to met-hemoglobin results in an acute hemolytic vascular inflammatory process causing
106 acute lung injury (30, 50). We hypothesize that the oxidation of hemoglobin during pneumococcal
107 disease can exacerbates cytotoxicity in the lungs but details of these oxidative reactions in cultures
108 of Spn strains are not available. Therefore, in this study we comprehensively investigated the
109 oxidation of hemoglobin by Spn cultures. We discovered that the oxidative capacity of Spn cultures,
110 under the culture conditions utilized here, was attributed to $H_2O_2$ produced through catalytic
111 reactions of SpxB but not to that of LctO. We also found that Spn-$H_2O_2$ caused the degradation of
112 heme and that a number of $H_2O_2$-producing, alpha-hemolytic, Streptococci oxidized hemoglobin and
113 degraded heme from hemoglobin. An *ex vivo* model of pneumococcal bacteremia further
114 demonstrated that oxidation of hemoglobin and heme degradation occurred rapidly and that heme,

115 but not hemoglobin or red blood cells, caused an upregulated transcription of *spxB*. Oxidative
116 reactions driven by Spn-$H_2O_2$ might contribute to the pathogenesis of pneumococcal disease and
117 can also be important for the symbiosis with other non-hydrogen peroxide producing bacteria by
118 providing nutrients such as heme-iron.
119
120 **Results**
121 ***Streptococcus pneumoniae*-produced hydrogen peroxide oxidizes heme-hemoglobin, causing the**
122 **loss of the Soret peak.** We demonstrated that the alpha and beta chains of oxy-hemoglobin are
123 deoxygenated by *S. pneumoniae* strains but further oxidation of heme-$Fe^{+2}$ was not investigated
124 (23). To assess this, Todd-Hewitt broth (THY) supplemented with sheep oxy-hemoglobin (oxyHb),
125 which contains heme-$Fe^{2+}$, was inoculated with TIGR4 and incubated at 37°C in a 5% $CO_2$ and ~20%
126 $O_2$ atmosphere. As a control, uninfected THY-oxyHb was incubated under the same conditions. After
127 30 min of incubation, TIGR4 cultures caused the shift of the Soret curve from heme-$Fe^{2+}$, that peaks
128 at 415 nm, to a Soret curve of heme-$Fe^{3+}$ at 405 nm (Fig. 1A). As expected, this hemoglobin
129 preparation was deoxygenated producing met-hemoglobin (Fig. 1B). Similar oxidation of heme-$Fe^{2+}$
130 to heme-$Fe^{3+}$ was observed when oxy-hemoglobin was purified from horse erythrocytes and
131 incubated with Spn strains TIGR4, or D39 (not shown). Cultures of THY-oxyHb inoculated with
132 hydrogen peroxide-deficient strain TIGR4Δ*spxB*Δ*lctO,* or D39Δ*spxB*Δ*lctO*, did not cause the shift of
133 the Soret curve (Fig. 1A and not shown). Hemoglobin in uninfected cultures was not auto-oxidized
134 after this 30 min incubation period (Fig. 1A).
135 Extended incubation of TIGR4 in THY-oxyHb revealed that the Soret curve was lost in a time-
136 dependent manner (Fig. 1C). To assess if Spn-$H_2O_2$ had caused the loss of the Soret peak, we
137 inoculated THY-oxyHb cultures with TIGR4Δ*spxB*Δ*lctO* and the culture was incubated for 6 h. A Soret

138 curve was observed in this culture but the heme-$Fe^{2+}$ peak (415 nm), observed after 30 min post-
139 inoculation (Fig. 1A), had shifted to 405 nm representing heme-$Fe^{3+}$ (Fig. 1D). The deoxygenation of
140 hemoglobin in THY-oxyHb cultures of TIGR4Δ*spxB*Δ*lctO* was, however, due to autoxidation because
141 uninfected cultures incubated under the same conditions at 37°C, and with a 5% $CO_2$ and ~20% $O_2$
142 atmosphere, had shifted to heme-$Fe^{3+}$ as well (Fig. 1C).

143 To further confirm that the loss of the Soret peak was due to Spn-$H_2O_2$, we prepared a
144 complemented strain by cloning back *spxB* and *lctO* (Ω*spxB*Ω*lctO*) between SP_1113 and SP_1114
145 (Fig. 2). We also complemented TIGR4Δ*spxB* with a single copy of *spxB* to be utilized later (Fig. 2).
146 This chromosomal location is unaffected by exogenous regulatory elements, such that
147 complementing genes were controlled by their own promoters and insertion of genes within
148 SP_1113 and SP_1114 did not affect virulence (51-54). Compared to wt and TIGR4Δ*spxB*Δ*lctO*,
149 complemented strains showed a slight but not significant growth delay (Fig. 2B); however $H_2O_2$
150 production was restored to wt levels, as assessed with the Prussian blue-forming reaction and the
151 Amplex Red kit (Fig. 2C and 2D) (55). In THY-oxyHb cultures of Ω*spxB*Ω*lctO* incubated for 6 h, the
152 Soret curve had flattened (Fig. 1D). These results suggest that Spn-$H_2O_2$ causes heme degradation.

153 Given that heme-$Fe^{2+}$ in THY-oxyHb cultures was oxidized to heme-$Fe^{2+}$ (Fig. 1A) prior to
154 losing the Soret curve (Fig. 1C), we next assessed if the oxidation state of heme was important for
155 the subsequent loss of the Soret curve. To investigate this, we supplemented THY with deoxy-
156 hemoglobin (i.e., met-hemoglobin) containing heme-$Fe^{3+}$ (THY-Hb) and the culture was incubated
157 with Spn. A similar loss of the Soret curve was observed with TIGR4 wt and Ω*spxB*Ω*lctO* (Fig. 1E),
158 but an intact curve was obtained in cultures of TIGR4Δ*spxB*Δ*lctO* (Fig. 1E), indicating that heme-$Fe^{3+}$
159 was further degraded. These results demonstrated that Spn-$H_2O_2$ converts oxyHb to metHb.

160

161 **Exogenous hydrogen peroxide supplementation at levels produced in *S. pneumoniae* cultures**
162 **recapitulates hemoglobin oxidation.** We then assessed whether a similar concentration of
163 hydrogen peroxide to that observed in wt cultures of Spn (<1 mM) [Fig. 2D and references (39, 40)]
164 can alter the heme-$Fe^{3+}$ curve. For easy comparison of the multiple concentrations utilized in this
165 experiment, we plotted the maximum absorbance obtained by spectroscopy for THY-Hb (405 nm)
166 and we compared against that of THY-Hb treated with an increasing concentration of hydrogen
167 peroxide. As shown in Fig. 1F, 10 µM hemoglobin in THY-Hb peaks at an absorbance of ~0.8. After 4
168 h of incubation with hydrogen peroxide, the absorbance was significantly reduced with a
169 concentration of 88 µM and above, including the concentration of hydrogen peroxide observed in
170 Spn cultures (~880 µM) (Fig. 1F). Altogether, these results indicate that the heme moiety in oxidized
171 hemoglobin is degraded by Spn-$H_2O_2$.
172
173 **Oxidation of hemoglobin in *S. pneumoniae* cultures is mainly caused by hydrogen peroxide**
174 **catalyzed through pyruvate oxidase SpxB.** Under aerobic conditions, hydrogen peroxide in
175 pneumococcal cultures is produced through catalytic reactions of pyruvate oxidase (SpxB) and
176 lactate oxidase (LctO) (43, 44). To assess the contribution of each enzyme, single Δ*spxB* or Δ*lctO*
177 prepared in the TIGR4, or EF3030, background were assessed in THY-Hb cultures. In cultures of wt
178 strains TIGR4, and EF3030, isogenic mutant TIGR4Δ*lctO*, and EF3030Δ*lctO*, Ω*spxB*Ω*lctO* and
179 TIGR4Δ*spxB*Ω*spxB* complemented strain the Soret Heme-$Hb^{3+}$ curve was flattened, causing a
180 statistically significant reduction of the 405 nm peak (Fig. 3A). In contrast, in THY-Hb cultures of
181 TIGR4Δ*spxB* or EF3030Δ*spxB,* the Soret curve remained intact, similar to THY-Hb cultures inoculated
182 with the corresponding Δ*spxB*Δ*lctO* mutant (Fig. 3A and 3B). Additional D39Δ*spxB*Δ*lctO,* or
183 D39Δ*spxB* strain (P878), hydrogen peroxide-deficient mutants did not alter the Soret curve while

184 D39Δ*spxB*/*spxB* complemented strain, P1221, caused the loss of the Soret curve (Fig. 3C). These
185 experiments demonstrated that oxidation of hemoglobin in cultures of Spn is mainly caused by
186 hydrogen peroxide sourced from reactions catalyzed by SpxB.
187
188 **Spn-produced $H_2O_2$ degrades heme-$Fe^{3+}$.** Heme degradation occurs through enzymatic reactions or
189 by nonselective destruction of heme double bonds caused by reactive oxygen species, such as $H_2O_2$
190 (35, 56). To investigate whether Spn-$H_2O_2$ caused degradation of heme, THY-Hb medium was
191 inoculated with TIGR4, EF3030, their hydrogen peroxide mutant derivatives, or complemented
192 strains and heme was assessed in supernatants using an in-gel heme assay (57, 58). Signal of heme,
193 heme-bound to hemoglobin monomers or dimers, was detected in uninfected THY-Hb cultures
194 incubated for 6 h (Fig. 4A). Heme signal in the supernatant of THY-Hb cultures incubated with TIGR4
195 for 2 h was similar to that of the uninoculated control but it decreased after 4 h post-inoculation
196 and was not detected 6 h post-inoculation (Fig. 4A). In THY-Hb cultures of TIGR4, TIGR4Δ*lctO*,
197 TIGR4Ω*spxB*Ω*lctO*, TIGR4Δ*spxB*Ω*spxB,* EF3030, or EF3030Δ*lctO* the signal of heme had already
198 disappeared after 6 h of incubation (Fig. 4B and 4C). In contrast, in THY-Hb cultures of
199 TIGR4Δ*spxB*Δ*lctO,* TIGR4Δ*spxB*, EF3030Δ*spxB*Δ*lctO*, or EF3030Δ*spxB*, signal of free heme, and heme-
200 bound to hemoglobin was detected, thus confirming that degradation of heme had occurred in
201 these cultures through hydrogen peroxide produced by SpxB.
202 As a loading control and to additionally investigate if hemoglobin had been degraded,
203 supernatants were probed by Western blot with a polyclonal anti-hemoglobin antibody. Our results
204 revealed a similar concentration of hemoglobin in those supernatants, confirming that the apo-
205 protein was not degraded after the 2, 4 or 6 h incubation period with Spn (Fig. 4A, bottom panel). As
206 expected since heme was degraded by Spn-$H_2O_2$, the intracellular concentration of iron was 79.19,

207 18.21, or 108.79 µM of Fe/µg of protein in TIGR4, TIGR4Δ*spxB*Δ*lctO* or TIGR4Ω*spxB*Ω*lctO*,
208 respectively, confirming that iron was released and taken by wt and complemented strain.
209 Altogether, these experiments demonstrated that Spn-$H_2O_2$ degrades free-heme and heme bound
210 to hemoglobin.
211
212 **Streptococci that produces hydrogen peroxide, but not other respiratory bacteria, causes the**
213 **degradation of heme.** Non-encapsulated Spn (NESpn) and other alpha-hemolytic streptococci
214 produce hydrogen peroxide (59, 60). We therefore assessed a collection of NESpn and oral
215 streptococci for heme degradation. We included *S. mutans* as an additional control since strains lack
216 production of $H_2O_2$ (61, 62). As shown in Fig. 5, degradation of heme-$Fe^{3+}$ was observed in THY-Hb
217 cultures of NESpn strains MNZ41, MNZ67 and *S. salivarius*, *S. mitis*, *S. pseudopneumonanie* and *S.*
218 *oralis* but not in cultures of *S. mutans* (Fig. 5A). We also tested cultures of other bacterial species
219 that cohabit the upper airways along with oral streptococci, such as *Haemophilus influenzae,*
220 *Staphylococcus aureus* and assessed cultures of *Klebsiella pneumoniae*. The incubation of THY-Hb
221 with any of these bacterial species did not cause heme degradation (Fig. 5A). Streptococcal species
222 that caused heme degradation produced hydrogen peroxide, while those unable to affect the heme-
223 hemoglobin Soret curve did not (Fig. 5B). Altogether, these experiments demonstrated that Spn and
224 other alpha hemolytic streptococci that produce abundant hydrogen peroxide, oxidizes hemoglobin
225 causing the degradation of heme.
226
227 **Heme is oxidized and degraded in an *ex-vivo* model of pneumococcal bacteremia.** During the
228 course of pneumococcal bacteremia erythrocytes are lysed by the pneumolysin (Ply), released
229 through autolysis (63). Ply is also located on the bacterial membrane where it lyses red blood cells

230 through contact (19, 20). Abundant Spn-$H_2O_2$ is produce as early as 2 h post-inoculation (Fig. 2D)
231 thereby we sought to assess whether oxidation of hemoglobin and heme degradation occur in an
232 *ex-vivo* model of pneumococcal bacteremia (Fig. 6A). To assess this, we supplemented THY broth
233 with a suspension of red blood cells (THY-RBC), and this medium was infected with TIGR4,
234 TIGR4Δ*ply*, or TIGR4Δ*spxB*Δ*lctO*. The oxidation and concentration of hemoglobin as well as heme
235 degradation were investigated.

236 As expected, the Soret curve was not observed in supernatants from non-lysed THY-RBC
237 control and it was also absent in THY-RBC supernatants infected with TIGR4Δ*ply,* because it does
238 not lyse erythrocytes (Fig. 6B). Given that RBCs contains oxy-hemoglobin (Hb-$Fe^{2+}$), the Soret curve
239 of the positive control, where RBC had been lysed with saponin, peaked at 415 nm with an average
240 absorbance of 1.38 (Fig. 6B). The concentration of cell-free hemoglobin in this control supernatant
241 was 17.35 µM as measured by the Quantichrom assay (Table 1). The Soret curve from THY-RBC
242 cultures infected with TIGR4 peaked at 405 nm with an average absorbance of 1.39 (Fig. 6B) and
243 concentration of hemoglobin of 12.8 µM (Table 1). These results indicate that maximum TIGR4-
244 induced release of hemoglobin is achieved within 30 min of incubation, compared with the saponin-
245 induced released control, and that the oxidation of heme-$Fe^{2+}$ to heme-$Fe^{3+}$ had already occurred
246 (Fig. 6B). Similar to the wt and because TIGR4Δ*spxB*Δ*lctO* produces Ply (21, 23), a Soret curve was
247 observed in THY-RBC cultures infected with this hydrogen peroxide deficient mutant as soon as 30
248 min post-inoculation (Fig. 6B). This Soret curve peaked at 415 nm with an average absorbance of
249 1.21 and a concentration of hemoglobin of 16.4 µM (Table 1), indicating that most hemoglobin had
250 been released but, unlike the wt strain, oxidation of heme-$Fe^{2+}$ did not occur because of the lack of
251 hydrogen peroxide. Accordingly, oxidation of hemoglobin did not occur in TIGR4 cultures treated

252 with catalase but it was oxidized to met-hemoglobin in TIGR4 cultures treated with protease
253 inhibitors (Fig. 6B).

254 After 6 h of incubation, autoxidation of uninoculated, saponin-released hemoglobin in THY-
255 RBC cultures (Fig. 6C, Hb-$Fe^{3+}$) and those infected with TIGR4 treated with catalase (Fig. 6C) were
256 oxidized. THY-RBC medium infected with TIGR4 had already flattened the heme-$Fe^{3+}$ curve and
257 therefore heme had been degraded but not in those of TIGR4 treated with catalase (Fig. 6C).
258 Degradation of heme was not inhibited by supplementing THY-RBC before the infection with
259 protease inhibitors (Fig. 6C). We next treated saponin-released oxy-hemoglobin with increasing
260 amounts of $H_2O_2$ and the oxidation to met-hemoglobin and then degradation of heme was
261 recapitulated (Fig. 6D). Altogether, our results indicate that oxidation of hemoglobin and
262 degradation of heme by Spn-$H_2O_2$ occur during pneumococcal bacteremia.

263 To further mimic bacteremia, we added THY with 10% of human serum and supplemented
264 this broth culture with 10 µM met-hemoglobin. In addition, non-diluted human serum was
265 supplemented with 10 µM met-hemoglobin. These hemoglobin-containing serum cultures were
266 infected with TIGR4 and incubated at different times. A time course degradation of met-hemoglobin
267 was observed in both culture conditions (Fig. 6E and 6F), confirming that hemoglobin is oxidized and
268 degraded when Spn growths in human serum.

269 Because the release of hemoglobin and its oxidation was observed early during the
270 simulated bacteremia (i.e., 30 min), to gain insights into the mechanism leading to hemoglobin
271 oxidation and heme degradation, we investigated expression of *ply*, *spxB,* and *lctO* during
272 incubation of Spn in THY-RBC, THY-Hb or in THY supplemented with heme. Compared to THY control
273 cultures, the expression of *ply, spxB,* and *lctO* did not significantly change when TIGR4 grew in broth
274 cultures added with RBCs or hemoglobin. However, transcription of *spxB* was upregulated when

275 TIGR4 was incubated in THY containing heme, whereas the transcription *lctO* and *ply* was
276 downregulated (Fig. 7). Together, these experiments indicate that under these culture conditions
277 heme was the inducer for Spn-$H_2O_2$ production.
278
279 **Discussion**
280 We have demonstrated in this study that $H_2O_2$ produced by the pneumococcus, Spn-$H_2O_2$,
281 and other alpha-hemolytic Streptococci, caused the oxidation of hemoglobin to met-hemoglobin
282 with a subsequent degradation of heme. The current study also demonstrated that the oxidation of
283 hemoglobin and heme degradation occurred in a simulated bacteremia infection suggesting that
284 these oxidative reactions may occur during pneumococcal disease.
285 *In vitro* oxidation of hemoglobin with hydrogen peroxide produces ferryl hemoglobin [Hb-
286 $Fe^{4+}$], a highly reactive form of hemoglobin that gets reduced to met-hemoglobin (64). With an
287 increased presence of hydrogen peroxide molecules, met-hemoglobin gets oxidized back to Hb-$Fe^{4+}$
288 , which in turn causes heme degradation (65). Iron stored in heme-hemoglobin is poorly reactive
289 but once freed up, as a consequence of heme degradation, free iron can react with hydrogen
290 peroxide to produce another highly reactive hydroxyl radical (66, 67). Indeed, we have
291 demonstrated that free iron present in THY medium is enough to generate hydroxyl radicals ($^{\bullet}OH$)
292 (40), killing *S. aureus* strains rapidly (39, 68, 69). The increase of iron in the culture medium due to
293 heme degradation should result in an increased generation of $^{\bullet}OH$ radicals. The potential presence
294 of two highly reactive radicals, Hb-$Fe^{4+}$ and $^{\bullet}OH$, for the cytotoxicity seen during pneumococcal
295 disease is being investigated in our laboratories.
296 It has been investigated that nearly 3% of oxy-hemoglobin is auto-oxidized inside
297 erythrocytes, and this auto-oxidation is caused by $2x10^{-7}$ mM of hydrogen peroxide generated in the

298 cytosol of red blood cells (70). Although auto-oxidation by $CO_2$ occurred in our *in vitro* system 4 h
299 post-inoculation (i.e., auto-oxidation was not observed when incubated at 37°C with no $CO_2$), Spn
300 cultures produce $10^7$-fold more (~1 mM) hydrogen peroxide within a few hours of incubation and
301 caused the rapid oxidation of hemoglobin leading to the release of heme, a toxic molecule, with its
302 subsequent degradation (65). We demonstrated that heme degradation caused an increased on
303 free-iron in the medium that was taken by pneumococci. These novel observations might have
304 important implications for pathogenesis of hydrogen peroxide-producing Streptococci but also for
305 the symbiosis observed in bacterial communities where some species can benefit from heme and
306 iron release by hydrogen peroxide-producing bacteria.
307
308 In children with SCD, hemoglobin (Hb)S is oxidized to Hb-$Fe^{4+}$ then reduced to met-
309 hemoglobin and resulting in an acute hemolytic vascular inflammatory process causing acute lung
310 injury (30, 50). Both Hb-$Fe^{4+}$ and met-hemoglobin induce a drop of mitochondrial oxygen
311 consumption and mitochondrial membrane potential in epithelial lung cells (36). Acute chest
312 syndrome is an important cause of hospitalization and mortality in children with SCD and Spn is a
313 leading etiologic agent of acute chest syndrome. While the precise role of Spn is still unclear, SCD
314 children are ~100-fold more susceptible to pneumococcal infection (71). Studies of the oxidation of
315 hemoglobin by Spn-$H_2O_2$, however, have been neglected. We recently demonstrated that the
316 growth of planktonic Spn, and formation of pneumococcal biofilms, is enhanced by supplementing
317 the culture medium with human hemoglobin (72, 73). Besides iron, other nutrients may become
318 accessible to pneumococcus, since the oxidation of hemoglobin by hydrogen peroxide releases
319 globin-derived peptides (29), but also a striking transcriptome remodeling was identified that

320 included upregulated transcription of genes encoding transporters of glyco-conjugated molecules
321 (72, 73).

322 Besides nutrients, oxidative reactions may lead to unintended consequences. During
323 pneumococcal pneumonia the pulmonary parenchyma presents with hemorrhage, inflammatory
324 congestion, hepatization, suppurative infiltration, and lung parenchymal injury (4, 9-13). Whereas
325 there are a number of virulence factors implicated in the pathophysiology of lung infection (63), the
326 oxidation of hemoglobin through Spn-$H_2O_2$ may also be an important contributor to pneumococcal
327 disease. For example, mice intranasally inoculated with Spn develop lung hemorrhage, at necropsy,
328 and histological analysis reveals lung consolidation associated with alveolar septal edema and
329 pleomorphic alveolar, interstitial, and perivascular cellular inflammation (74). Spn mutants in the
330 *spxB* gene whether with a pleotropic capsule defect or not, were attenuated for virulence in mouse
331 models of pneumococcal disease (46, 47, 75).

332 There are other important implications as a result of the oxidation of hemoglobin by
333 hydrogen peroxide produced by streptococci. Heme release and/or heme degradation through,
334 hydrogen peroxide, may be beneficial to other bacteria which do not synthetize large amounts of
335 this pro-oxidant but that require iron for their metabolism and pathogenesis. For instance, it has
336 been recently demonstrated that dental plaque bacteria such as *S. gordonii*, which produces
337 hydrogen peroxide, oxidizes hemoglobin to release heme, and this free-heme facilitates the
338 colonization of the dental plaque by a Gram-negative strain *Porphyromonas gingivalis* (49). *P.*
339 *gingivalis* does not produce siderophores but it has a sophisticated mechanism for heme-iron
340 acquisition (76). Conversion of oxy-hemoglobin to met-hemoglobin, by hydrogen peroxide
341 producing bacteria, allows the release of heme that can be taken by these microorganisms.

342 In summary, we demonstrated that Spn and other hydrogen peroxide-producing
343 Streptococci, oxidizes hemoglobin from human and other species, releasing and degrading heme.
344 These oxidative reactions occurred early during the lag phase of growth indicating that metabolic
345 adaptation for growth in the presence of hemoglobin stimulated production of Spn-$H_2O_2$. This
346 upregulated metabolic adaption was the result in part of the release of heme since gene expression
347 studies demonstrated an upregulation of *spxB* transcription but not that of *lctO* or the pneumolysin
348 gene *ply*, under the culture conditions tested. Noteworthy, incubation with erythrocytes or
349 hemoglobin did not induced a regulation of *spxB* in the current study. We have observed a potential
350 toxic radical produced during the oxidation of hemoglobin, spanning the incubation time utilized in
351 gene expression studies, that may explain the observed downregulation of *spxB* (Scasny et al,
352 unpublished observations). Efforts are in place to assess the specific role for these oxidative
353 reactions for pathogenesis and bacterial symbiosis.
354

355 **Material and Methods**

356 **Bacterial strains, material, and growth conditions**. All Spn wild type strains and mutant derivatives
357 used in this study are listed in Table 2. Bacterial stocks were prepared in medium containing skim
358 milk-tryptone-glucose-glycerin (STGG) and stored at -80°C (77). Pneumococci were rotinously
359 cultivated at 37°C in a 5% $CO_2$ and ~20% $O_2$ atmosphere on blood agar plate (BAP). Non-typeable
360 *Haemophilus influenzae* (NTHI) was grown on chocolate agar plate (CAP), which was prepared with
361 heat-lysed horse blood, a source of hemin and NAD. *Klebsiella pneumoniae* and *Staphylococcus*
362 *aureus* were cultivated on tryptic soy agar (TSA). Experiments were performed using Todd-Hewitt-
363 broth with 0.5% yeast extract (THY), THY added with 10 µM human met-hemoglobin (Sigma-
364 Aldrich), THY added with 5 µM heme (Sigma-Aldrich), THY added with sheep erythrocytes (Quad

365 Five), and horse erythrocytes (Lampire). In experiments inoculated with NTHI, THY medium was
366 supplemented with hemin (10 µg/ml), and NAD (2 µg/ml). Brain heart infusion (BHI) broth, Bacto
367 agar, Bacto Tryptic Soy Broth, Bact Yeast Extract and Bacto Todd Hewitt Broth were purchased from
368 Becton, Dickinson and Company. Antibiotics utilized were gentamycin, erythromycin,
369 spectinomycin, chloramphenicol, and were all sourced from Sigma-Aldrich. Hydrogen peroxide
370 (Fisher Scientific), Nicotinamide adenine dinucleotide (NAD(+)) (Sigma-Aldrich), Catalase (Sigma-
371 Aldrich), Complete™, Mini Protease Inhibitor Cocktail (Roche), $FeCl_3 \cdot 6H_2O$ and potassium
372 hexacyanoferrate (III) (Sigma-Aldrich), o-dianisidine (Alfa Aesar) /sodium acetate (Sigma-Aldrich),
373 ethanol and methanol (Fisher Scientific). Human serum was purchased from MP Biomedicals.

374 **Preparation of inoculum for experiments.** The inoculum was prepared as previously described (40).
375 Briefly, bacteria were inoculated on blood agar plates (BAP) and incubated overnight at 37°C in a 5%
376 $CO_2$ atmosphere. Bacteria were then harvested from plates by PBS washes and this suspension was
377 used to inoculate THY with or without additives, that was brought to a final $OD_{600}$ of ~0.1. This
378 suspension contained ~$5.15 \times 10^8$ cfu/ml as confirmed by dilution and platting of aliquots of the
379 suspension.

380 **Bacterial broth culture medium containing oxy-hemoglobin.** Sheep or horse erythrocytes were
381 washed three times with sterile PBS (pH=7.4) at 300 × *g* for 5 min in a refrigerated centrifuge
382 (Eppendorf). These washed erythrocytes suspension was lysed with 0.1% saponin and the
383 concentration of oxy-hemoglobin in this preparation was determined using the QuantiChrom™
384 Hemoglobin Assay Kit (BioAssay Systems); oxy-hemoglobin was then added to THY broth to a final
385 concentration of ~10 µM. The concentration, and redox state of oxy-hemoglobin was verified by
386 spectroscopy before each experiment. In some experiments, THY containing oxy-hemoglobin was

387 supplemented with an excess of catalase to a final concentration of 400 U/ml, or with 1X complete
388 protease inhibitors cocktail (Roche).

389 **Studies of the oxidation of oxy-hemoglobin, met-hemoglobin and heme degradation by**
390 **spectroscopy.** Experiments were conducted using six-well microplates (Genesee Scientific) added
391 with THY containing a 2% suspension of washed sheep erythrocytes, 10 µM of oxy-hemoglobin, or
392 10 µM of met-hemoglobin. In some experiments human serum was supplemented with 10 µM of
393 met-hemoglobin, or THY was supplemented with human serum to a final 10% concentration (v/v)
394 and added with 10 µM of met-hemoglobin. These media were inoculated with Spn or the other
395 bacterial species listed in each experiment, and incubated for the indicated time at 37°C in a 5% $CO_2$
396 and ~20% $O_2$ atmosphere. At the of the incubation time, supernatants containing planktonic
397 bacteria were removed from cultures and bacteria were pelleted down by centrifugation at 13,000
398 rpm x 5 min in a refrigerated micro-centrifuge (Eppendorf). In another set of experiments, THY
399 containing 10 µM of human met-hemoglobin was treated with different concentrations of hydrogen
400 peroxide for 6 h. The oxidation of oxy-hemoglobin to met-hemoglobin and further oxidation and
401 degradation of met-hemoglobin was determined by analyzing the spectra spanning 200 nm through
402 1000 nm in bacteria-free supernatants, using a spectrophotometer Omega BMG LabTech
403 (ThermoFisher).

404 **Quantification of hydrogen peroxide production.** Hydrogen peroxide production was quantified
405 from bacterial cultures inoculated in six-well microplates (Genesee Scientific) that had been added
406 with THY. These cultures were incubated at 37°C in a 5% $CO_2$ and ~20% $O_2$ atmosphere for the
407 indicated time. At the end of the incubation, the culture supernatant was collected, centrifuged at
408 4°C for 5 min at 15,000 rpm and then the supernatant was transferred to a new tube and kept in ice
409 for no more than 30 min. Some supernatants were filtered sterilized using a 0.4 µm syringe filter

410 (Fisher scientific). Collected supernatants were diluted with 1× reaction buffer of the Amplex Red
411 $H_2O_2$ assay kit (Molecular Probes), and hydrogen peroxide levels were quantified according to the
412 manufacturer's instructions using a spectrophotometer Omega BMG LabTech (ThermoFisher).

413 **Qualitative detection of hydrogen peroxide production by *S. pneumoniae* strains.** Qualitative
414 detection of $H_2O_2$ production by Spn was performed using the Prussian blue agar assay, which limit
415 of detection is 2.5 nm $H_2O_2$ (55). Prussian blue agar plates were made with 1.0 g/liter of $FeCl_3 \cdot 6H_2O$,
416 1.0 g/liter of potassium hexacyanoferrate III ($K_3[Fe(CN)_6]$) also known as Prussian blue, 37 g/liter of
417 dehydrated BHI broth, and 15 g/liter of agar. Prior to experiments, detection of $H_2O_2$ was assessed
418 by dropping 10 µl of a 1 mM $H_2O_2$ solution that reduced $K_3[Fe(CN)_6]$ and causing its precipitation and
419 then a blue halo within minutes. PBS was used as a negative control. Spn strains or culture
420 supernatants (10 µl) obtained as described above, were inoculated, or spotted, respectively, onto
421 Prussian Blue agar plates. These plates were incubated at 37 °C in a 5% $CO_2$ and ~20% $O_2$
422 atmosphere overnight (Spn) or for 2 h (supernatants) after which plates were photographed with a
423 Canon Rebel EOS T5 camera system and digital pictures were analyzed.

424 **Western blotting.** Bacteria were grown in THY with 10 µM hemoglobin at 37°C for 2 h, 4 h, and 6 h.
425 After incubation the cells were harvested by centrifuge at 15,000 rpm for 5 min and the supernatant
426 were transferred to new tube. The collected samples were combined with 4x reducing sample
427 buffer and boiled 5 minutes. The mixture was loaded into 10 well 4-12% Mini-PROTEAN® TGX™
428 precast gel (Biorad), and run 2 hours at 90 V in running buffer. Gels were transferred to
429 nitrocellulose membranes in transfer buffer supplemented with 20% ethanol with Trans-Blot Turbo
430 Transfer System. Membranes were blocked 1 h at room temperature in 5% non-fat dry milk in TBS
431 supplemented with 0.1% Tween-20 (TBST). Then a membrane was incubated with the Hb polyclonal
432 antibody (Invitrogen) at 1:1000 dilution in 5% non-fat dry milk in TBST overnight at 4°C. Next day,

433 the blot was washed 3x 5 min with TBST, and incubated with donkey anti-goat IgG-HRP (Santa Cruz)
434 secondary antibody 1:5000 in 5% non-fat dry milk in TBST 1 h at room temperature. Blots were
435 washed 3x 5 min in TBST and 2mL each SuperSignal Substrate (Thermo Fisher Scientific) reagent was
436 added to blot and incubated for 5 min at room temperature. Blots were imaged on a ChemiDoc MP
437 (BioRad) using ImageLab 5.0 software, automatic exposure settings for Chemiluminescence, high
438 specificity, optimizing for bright bands.

439 **In-gel heme staining.** Bacteria were grown in THY with 10 µM hemoglobin at 37°C for 2, 4, or 6 h,
440 after which supernatants were collected, spun down and combined with non-reducing loading
441 buffer. The mixtures were loaded into a non-denaturing 12% Mini-PROTEAN® TGX™ precast gel
442 (Biorad), and run for 2 h at 90 V in running buffer lacking SDS. The gel was then stained using a
443 published protocol (35). Briefly, after electrophoresis gels were immersed into a methanol/sodium
444 acetate (pH=5) solution and incubated at room temperature on rocking platform (VWR) at 1 speed
445 for 2 min with constant shaking. After incubation, the gel was added with a solution of o-
446 dianisidine/sodium acetate (pH=5)and incubated for 20 min in the dark. To visualize heme in the
447 gel, 3% hydrogen peroxide was added, and the reaction was stopped by washing with distilled
448 water. The gel was then photographed with a Canon Rebel EOS T5 camera system and digital
449 pictures were analyzed.

450 **RNA extraction and qRT-PCR analysis.** Bacteria were inoculated into THY, or THY containing 5 µM
451 heme, 5 µM Hb, or a 1% suspension of RBC and incubated at 37°C for 2 h. After incubation the
452 bacterial suspension was collected, and mixed with RNAprotect Reagent (Qiagen). Then cells were
453 harvested and the total RNA was extracted using the RNeasy mini kit (Qiagen) following the
454 manufacturer's instruction. DNA was removed using the Turbo DNase-free kit (Life Technologies).
455 The RNA concentration was obtained using a NanoDrop spectrophotometer (Thermo Fisher

456 Scientific), and 200 ng of RNA were cDNA transcribed using the iScript™ cDNA Synthesis Kit (Biorad).
457 Gene expression analysis was carried out using the PerfeCTa SYBR® Green SuperMix (Quantabio)
458 and CFX96 Touch Real-Time PCR system (Biorad). Primers used for the qRT-PCR analysis are listed in
459 Table 3. The following conditions were utilized: 1 cycle at 95°C for 3 min and 40 cycles of 95°C for 15
460 s, 60°C for 30 s and 72°C for 30 s. Melting curves were generated to confirm the absence of primer
461 dimers. The relative quantitation of mRNA expression was normalized to the constitutive expression
462 of the housekeeping 16S rRNA gene and calculated by the comparative CT ($2^{-\Delta\Delta CT}$) method (78).
463 **Preparation of *lctO* mutation in Spn strains EF3030 and D39.** To prepare an isogenic *lctO* mutant,
464 we PCR-amplified, using primers lcto-spec1 and lcto-spec2 (Table 3), an insertionally inactivated
465 *lctO*-spectinomycin fragment from strain TIGR4Δ*lctO* (40). This PCR product was purified using the
466 QIAquick PCR purification kit (Qiagen) and then transformed into EF3030 or D39 using an standard
467 transformation procedure (79). Transformants were harvested in BAP with spectinomycin
468 (100 µg/ml) and the insertional inactivation of *lctO* was confirmed by PCR with primers lcto-spec1 /
469 lcto-spec2 and sequencing.
470 **Construction of complemented strains.** To complement *spxB*, or *spxB* and *lctO,* into TIGR4Δ*spxB* or
471 TIGR4Δ*spxB*Δ*lctO*, respectively, we chose a 'neutral' chromosomal location within the *hplA* gene
472 (SP1113) in which insertions do not affect virulence (52). A *spxB* complemented fragment was
473 prepared by amplifying an upstream region carrying a fragment of the *hlpA* gene, using as a
474 template DNA purified from TIGR4, and primers hlpA-up1 and hlpA-up2 (Table 3). We then
475 generated a PCR fragment, using DNA purified from TIGR4 as a template, containing the *spxB* gene
476 and its promotor with primers spxB1 and spxB2 (Table 3). A downstream fragment containing the
477 *catP* gene from chloramphenicol resistance and a fragment of ORF SP1114 was amplified using as a
478 template DNA from strain JWV500 using primers hplA-down1 and hlpA-down2. PCR products were

479 purified using a QIAquick PCR purification kit (Qiagen) and ligated by splicing overlap extension PCR
480 with primers hlpA-up1/hlpA-down2. The PCR-ligated product was verified in a 0.8% DNA gel,
481 purified from the gel using QIAquick Gel Extraction Kit (Qiagen) and re-amplified by PCR with
482 primers hlpA-up1 and hlpA-down2. This PCR product was purified as above and used to transform
483 TIGR4Δ*spxB* using a standard procedure (79). Transformants were harvested in BAP plates
484 containing chloramphenicol (5 µg/ml) and screened by PCR using primers spxB1/spxB2 to confirm
485 the complementation of *spxB*.

486 To construct a *spxB* and *lctO* complemented strain, an upstream DNA fragment containing
487 *hlpA* and *spxB* was amplified using DNA purified from TIGR4Δ*spxB*Ω*spxB* and primers hlpA1 and
488 spxB2. Then, a DNA fragment was prepared by PCR amplification of the *lctO* gene and its putative
489 promotor region using TIGR4 DNA as a template and primers lctO1 and lctO2. The downstream
490 fragment containing the *catP* gene and a fragment of ORF SP1114 was used as prepared above.
491 After purification with a QIAquick PCR purification kit (Qiagen), these three DNA fragments were
492 ligated by splicing overlap extension PCR with primers hlpA-up1/hlpA-down2 and purified. This
493 construct was re-amplified with primers hlpA-up1 and hlpA-down2, purified and transformed into
494 TIGR4Δ*spxB*Δ*lctO*. Transformants were screened by PCR using primers hlpA-up1/hlpA-down2and
495 selected completed clones were further confirmed by $H_2O_2$ production.

496 **Metal content analysis.** Pneumococcal biofilms cultured in THY-Hb for 4 h were washed 3x with
497 ice-cold PBS, resuspended in 1 ml PBS and sonicated at high intensity for 5 min in 30 s on 30 s off
498 cycles using a Bioruptor (Diagenode, Denville, NJ, USA). Protein was determined in all samples by
499 the Bradford method and a known mass of sample was mineralized in concentrated $HNO_3$ trace
500 metal grade (Thermo Fisher Scientific) as previously described (80). Iron in each sample was
501 determined by atomic absorbance spectroscopy (AAS) using a flame 55 AA Absorption Spectrometer

502 (Agilent, Santa Clara, CA, USA). Analytical grade standards for iron (Thermo Fischer Scientific) were
503 diluted in 18ΩV water. The iron content on each sample was normalized to the initial mass of
504 protein as previously reported for other metals (81, 82).

505 **Statistical analysis.** We performed one-way analysis of variances (ANOVA) followed by Dunnet's
506 multiple comparison test, when more than two groups were compared or the Student *t* test to
507 compare two groups, as indicated. All statistical analysis was performed using the software Graph
508 Pad Prism (version 8.3.1).

509

510 **Figure legends**

511 **Fig. 1. Hydrogen peroxide produced in *S. pneumoniae* cultures oxidizes human hemoglobin.**
512 TIGR4, TIGR4Δ*spxB*Δ*lctO,* or TIGR4Ω*spxB*Ω*lctO* was inoculated in THY containing oxy-hemoglobin
513 [Hb ($Fe^{+2}$)] or met-hemoglobin [Hb ($Fe^{+3}$)], or left uninfected, and cultures were incubated for (A-B)
514 30 min, (C) 2 h or 6 h, (D-F) 6 h at 37°C in a 5% $CO_2$ atmosphere. Supernatants were collected
515 and the spectra were obtained using a spectrophotometer Omega BMG LabTech. Panel B shows the
516 enclosed area in A, corresponding to the absorbance peaks of the alpha chain and the beta chain of
517 oxy-hemoglobin, flattened in met-hemoglobin. In (A, B and E) the dotted lines indicate the Soret
518 peak for oxy-hemoglobin (415 nm) or met-hemoglobin (405 nm). (F) THY supplemented with met-
519 hemoglobin (Hb-$Fe^{3+}$) was added with the indicated concentration of hydrogen peroxide, or left
520 untreated. These cultures were incubated for 6 h at 37°C in a 5% $CO_2$ atmosphere after which the
521 supernatants were purified and the spectra were obtained as above. The absorbance at 405 nm
522 obtained for each assessed concentration, was utilized to construct the graphic. Error bars in all
523 panels represent the standard errors of the means calculated using data from at least three

524 independent experiments performed with two technical replicates. In (B-F) One-way ANOVA with
525 Dunnet's test for multiple comparison was performed, *$p$<0.05 compared against the Soret peak of
526 uninfected THY-Hb-$Fe^{2+}$ (B and D), uninfected THY-Hb-$Fe^{2+}$ and incubated 2 h (C) or uninfected THY-
527 Hb-$Fe^{3+}$(E and F).

528 **Fig. 2. Preparation of a TIGR4Δ*spxB*Δ*lctO*-derivative complemented strain carrying *spxB* and *lctO***
529 **or *spxB*.** (A) Schematic diagram showing the chromosomal region where *spxB* and *lctO* (top) or *spxB*
530 (bottom) was complemented in TIGR4Δ*spxB*Δ*lctO*, to create TIGR4Ω*spxB*Ω*lctO*, TIGR4Ω*spxB*.
531 Promotor regions of each gene (P) are indicated as well as terminators (†); gene IDs were included
532 using TIGR4 nomenclature. (B-D) TIGR4, TIGR4Δ*spxB*Δ*lctO*, TIGR4Ω*spxB*Ω*lctO*, or TIGR4Ω*spxB* was
533 inoculated in THY and incubated at 37°C in a 5% $CO_2$ atmosphere. (B) The $OD_{600}$ of the cultures was
534 obtained at the indicated time. Error bars represent the standard errors of the means calculated
535 using data from at least three independent experiments performed with two technical replicates.
536 (C) Supernatants from 4 h cultures were sterilized and an aliquot was inoculated onto Prussian-blue
537 agar plates (55) and the plates were incubated 2 h at room temperature after which they were
538 photographed. This experiment was repeated at least three times. (D) Hydrogen peroxide was
539 quantified from these supernatants using the Amplex Red assay. Error bars represent the standard
540 errors of the means calculated using data from two independent experiments performed with two
541 technical replicates. Limit of detection=0.56 µM.

542 **Fig. 3. Oxidation of hemoglobin occurs through hydrogen peroxide produced through SpxB**
543 **activity but not LctO.** (A) TIGR4, TIGR4Δ*spxB*Δ*lctO*, TIGR4Δ*spxB*, TIGR4Δ*lctO*, TIGR4Ω*spxB*Ω*lctO*, or
544 TIGR4Ω*spxB* or (B) EF3030, EF3030Δ*spxB*Δ*lctO*, EF3030Δ*spxB*, or EF3030Δ*lctO*, or (C) D39,
545 D39Δ*spxB*Δ*lctO*, D39 Δ*spxB*, or D39 Δ*spxB*/*spxB* were inoculated in THY containing met-
546 hemoglobin [Hb ($Fe^{3+}$)] and cultures were incubated for 4 h at 37°C in a 5% $CO_2$ atmosphere.

547 Supernatants were collected and the spectra were obtained using a spectrophotometer Omega
548 BMG LabTech. The absorbance at 405 nm obtained from each assessed strain, was utilized to
549 construct the graphics. Error bars in all panels represent the standard errors of the means calculated
550 using data from at least three independent experiments performed with two technical replicates
551 each. One-way ANOVA with Dunnet's test for multiple comparison was performed; NS=not
552 significant compared to THY-Hb ($Fe^{3+}$), *$p$<0.0001 compared with untreated THY-Hb ($Fe^{3+}$), or
553 Δ*spxB*Δ*lctO*, or Δ*spxB*; **$p$<0.003 compared with untreated THY-Hb ($Fe^{3+}$).

554 **Fig. 4. Oxidation of human hemoglobin by Spn-$H_2O_2$ leads to heme degradation.** (A-C) The samples
555 were stained by an in-gel staining method. (A) TIGR4 wt was inoculated in THY supplemented with
556 met-hemoglobin (THY-Hb) and incubated for 2, 4 or 6 h at 37°C in a 5% $CO_2$ atmosphere.
557 Supernatant was harvested and run in a 12% polyacrylamide gel under non-denaturing conditions
558 and heme was stained by an in-gel heme staining procedure. Free heme, heme-bound to
559 hemoglobin monomer (Hb-monomer) or to hemoglobin dimers (Hb-dimer), and the observed
560 molecular size in kDa, are indicated. In the bottom panel, supernatants were Western blotted using
561 a polyclonal anti-hemoglobin antibody. (B) TIGR4, TIGR4Δ*spxB*Δ*lctO*, TIGR4Δ*lctO*, TIGR4Δ*spxB*,
562 TIGR4Ω*spxB*, TIGR4Ω*spxB*Ω*lctO*, or (C) EF3030 wt strains or EF3030Δ*spxB*Δ*lctO*, EF3030Δ*spxB*, or
563 EF3030Δ*lctO*, was inoculated into THY-Hb and incubated for six hours. Supernatants were harvested
564 and analyzed as in (A).

565 **Fig. 5. Oxidation of hemoglobin occurs in cultures of oral Streptococci that produce hydrogen**
566 **peroxide.** THY supplemented with met-hemoglobin (THY-Hb) was left uninoculated or inoculated
567 with the indicated strain and incubated for 4 h at 37°C in a 5% $CO_2$ atmosphere. Supernatants were
568 collected and the spectra were obtained using a spectrophotometer Omega BMG LabTech. The
569 absorbance obtained at 405 nm for each assessed strain, was utilized to construct the graphic. Error

570 bars represent the standard errors of the means calculated using data from at least three
571 independent experiments performed with two technical replicates. One-way ANOVA with Dunnet's
572 test for multiple comparison was performed, *$p$<0.05, or NS=not significant, compared with
573 untreated THY-Hb. (B) Hydrogen peroxide was quantified from 4 h culture supernatants of each
574 strain and using the Amplex Red assay. Error bars represent the standard errors of the means
575 calculated using data from two independent experiments performed with two technical replicates.
576 Limit of detection=0.56 µM.

577 **Fig. 6. Hemoglobin is oxidized by Spn-$H_2O_2$ in an *ex vivo* bacteremia model with erythrocytes.** (A)
578 Model of *ex vivo* pneumococcal bacteremia showing pneumococci with pneumolysin (Ply) located in
579 the membrane; Ply also gets released through autolysis. Membrane-permeable hydrogen peroxide
580 ($H_2O_2$) is produced as a by-product of the oxidation of pyruvate. Bottom panel, oxy-hemoglobin (Hb-
581 $Fe^{2+}$) is then release from erythrocytes by Ply-induced erythrocyte lyses and once released, oxy-
582 hemoglobin gets oxidized by Spn-$H_2O_2$ to met-hemoglobin (Hb-$Fe^{3+}$). Alternatively, top panel, Spn-
583 $H_2O_2$ permeates inside erythrocytes causing the oxidation of hemoglobin that is then released from
584 lysed erythrocytes as met-hemoglobin (Hb-$Fe^{3+}$). (B and C) A suspension (2%) of sheep erythrocytes
585 in THY was inoculated with TIGR4, TIGR4 supplemented with catalase, TIGR4 supplemented with
586 protease inhibitors (PI), TIGR4Δ*spxB*Δ*lctO*, or TIGR4Δ*ply* and the inoculated cultures were incubated
587 for 30 min (B) or 6 h (C) at 37°C in a 5% $CO_2$ atmosphere. As a control, erythrocytes were lysed with
588 saponin and oxy-hemoglobin (THY-$Hb^{2+}$), that was released into the supernatant, was considered as
589 maximum hemoglobin release. (D) Oxy-hemoglobin was left untreated (Hb-$Fe^{2+}$) or added with
590 added with $H_2O_2$ and incubated for 6 h.(E and F) Human serum was supplemented with 10 µM met-
591 hemoglobin (HS+$Hb^{3+}$) or serum was used to supplement THY to a final 10% (v/v) and added with 10
592 µM met-hemoglobin (10% HS+$Hb^{3+}$). These media were inoculated with TIGR4 and incubated for 2,

593 4 or 6 h. Supernatants from experiments in panels (B-F) were collected and the spectra were
594 obtained using a spectrophotometer Omega BMG LabTech. In panels B through F, error bars
595 represent the standard errors of the means calculated using data from at least three independent
596 experiments. One-way ANOVA with Dunnet's test for multiple comparison was performed, *$p$<0.05,
597 or NS=not significant, compared with (B and C) TIGR4/catalase, (D) untreated Hb-$Fe^{2+}$, (E) untreated
598 10% HS+$Hb^{3+}$, or (F) untreated HS+$Hb^{3++}$.

599 **Fig. 7. Regulation of *ply*, *spxB* and *lctO* genes by incubation with erythrocytes, hemoglobin, or heme.** TIGR4
600 wt was inoculated in THY broth alone, in THY broth containing 1% sheep erythrocytes, THY with 10
601 µM hemoglobin (Hb) or THY with 5 µM heme. Cultures were incubated for 2 h at 37°C in a 5% $CO_2$
602 atmosphere, bacteria were then harvested, and RNA was extracted from these cultures and utilized
603 as template in qRT-PCR reactions with primers that amplified the *ply*, *spxB*, or *lctO* gene. Average $C_T$
604 values were normalized to the 16S rRNA gene, and the fold differences, relative to THY control,
605 were calculated using the comparative $C_T$ method ($2^{-\Delta\Delta C_T}$)(78).

606

607 **Acknowledgements**

608 This study was supported in part by a grant from the National Institutes of Health (NIH;
609 5R21AI144571-03) to JEV and Wesleyan University institutional funds to TP-B. BA was supported by
610 a Fulbright scholarship awarded by the US Department of State. FMF is supported by the Ronald E.
611 McNair Postbaccalaureate Fellowship program. The content is solely the responsibility of the
612 authors and does not necessarily represent the official view of the NIH or the US Department of
613 State. The authors thank Jaime Carrazco-Carrillo from Wesleyan University for his assistance in
614 some laboratory assays.

615

616

617 **References**

618 1. Jedrzejas MJ. 2001. Pneumococcal virulence factors: structure and function. Microbiol Mol
619 Biol Rev 65:187-207.
620 2. Kadioglu A, Weiser JN, Paton JC, Andrew PW. 2008. The role of *Streptococcus pneumoniae*
621 virulence factors in host respiratory colonization and disease. Nat Rev Microbiol 6:288-301.
622 3. Tomasz A. 2000. *Streptococcus pneumoniae* : molecular biology & mechanisms of disease.
623 Mary Ann Liebert, Inc., Larchmont, NY.
624 4. van der Poll T, Opal SM. 2009. Pathogenesis, treatment, and prevention of pneumococcal
625 pneumonia. Lancet 374:1543-56.
626 5. Klugman KP, Madhi SA, Albrich WC. 2008. Novel approaches to the identification of
627 *Streptococcus pneumoniae* as the cause of community-acquired pneumonia. Clin Infect Dis
628 47 Suppl 3:S202-6.

629 6. O'Brien KL, Wolfson LJ, Watt JP, Henkle E, Deloria-Knoll M, McCall N, Lee E, Mulholland K,
630 Levine OS, Cherian T. 2009. Burden of disease caused by *Streptococcus pneumoniae* in
631 children younger than 5 years: global estimates. Lancet 374:893-902.
632 7. Walker CL, Rudan I, Liu L, Nair H, Theodoratou E, Bhutta ZA, O'Brien KL, Campbell H, Black
633 RE. 2013. Global burden of childhood pneumonia and diarrhoea. Lancet 381:1405-16.
634 8. Holyoake LV, Hunt S, Sanguinetti G, Cook GM, Howard MJ, Rowe ML, Poole RK, Shepherd M.
635 2016. CydDC-mediated reductant export in Escherichia coli controls the transcriptional
636 wiring of energy metabolism and combats nitrosative stress. Biochem J 473:693-701.
637 9. Chao Y, Marks LR, Pettigrew MM, Hakansson AP. 2014. Streptococcus pneumoniae biofilm
638 formation and dispersion during colonization and disease. Front Cell Infect Microbiol 4:194.
639 10. Simell B, Auranen K, Kayhty H, Goldblatt D, Dagan R, O'Brien KL, Pneumococcal Carriage G.
640 2012. The fundamental link between pneumococcal carriage and disease. Expert Rev
641 Vaccines 11:841-55.
642 11. Eurich DT, Marrie TJ, Minhas-Sandhu JK, Majumdar SR. 2017. Risk of heart failure after
643 community acquired pneumonia: prospective controlled study with 10 years of follow-up.
644 BMJ 356:j413.
645 12. Musher DM, Rueda AM, Kaka AS, Mapara SM. 2007. The association between pneumococcal
646 pneumonia and acute cardiac events. Clin Infect Dis 45:158-65.
647 13. Masters IB, Isles AF, Grimwood K. 2017. Necrotizing pneumonia: an emerging problem in
648 children? Pneumonia (Nathan) 9:11.
649 14. Brown AO, Millett ER, Quint JK, Orihuela CJ. 2015. Cardiotoxicity during invasive
650 pneumococcal disease. Am J Respir Crit Care Med 191:739-45.

651 15. Brissac T, Shenoy AT, Patterson LA, Orihuela CJ. 2018. Cell Invasion and Pyruvate Oxidase-
652 Derived H2O2 Are Critical for Streptococcus pneumoniae-Mediated Cardiomyocyte Killing.
653 Infect Immun 86.
654 16. Nishimoto AT, Rosch JW, Tuomanen EI. 2020. Pneumolysin: Pathogenesis and Therapeutic
655 Target. Front Microbiol 11:1543.
656 17. Rubins JB, Duane PG, Charboneau D, Janoff EN. 1992. Toxicity of pneumolysin to pulmonary
657 endothelial cells in vitro. Infect Immun 60:1740-6.
658 18. Rubins JB, Duane PG, Clawson D, Charboneau D, Young J, Niewoehner DE. 1993. Toxicity of
659 pneumolysin to pulmonary alveolar epithelial cells. Infect Immun 61:1352-8.
660 19. Price KE, Greene NG, Camilli A. 2012. Export requirements of pneumolysin in Streptococcus
661 pneumoniae. J Bacteriol 194:3651-60.
662 20. Shak JR, Ludewick HP, Howery KE, Sakai F, Yi H, Harvey RM, Paton JC, Klugman KP, Vidal JE.
663 2013. Novel role for the Streptococcus pneumoniae toxin pneumolysin in the assembly of
664 biofilms. mBio 4:e00655-13.
665 21. Bryant JC, Dabbs RC, Oswalt KL, Brown LR, Rosch JW, Seo KS, Donaldson JR, McDaniel LS,
666 Thornton JA. 2016. Pyruvate oxidase of Streptococcus pneumoniae contributes to
667 pneumolysin release. BMC Microbiol 16:271.
668 22. Jacques LC, Panagiotou S, Baltazar M, Senghore M, Khandaker S, Xu R, Bricio-Moreno L, Yang
669 M, Dowson CG, Everett DB, Neill DR, Kadioglu A. 2020. Increased pathogenicity of
670 pneumococcal serotype 1 is driven by rapid autolysis and release of pneumolysin. Nat
671 Commun 11:1892.

672 23. McDevitt E, Khan F, Scasny A, Thompson CD, Eichenbaum Z, McDaniel LS, Vidal JE. 2020.
673 Hydrogen Peroxide Production by Streptococcus pneumoniae Results in Alpha-hemolysis by
674 Oxidation of Oxy-hemoglobin to Met-hemoglobin. mSphere 5.
675 24. Aprianto R, Slager J, Holsappel S, Veening JW. 2018. High-resolution analysis of the
676 pneumococcal transcriptome under a wide range of infection-relevant conditions. Nucleic
677 Acids Res 46:9990-10006.
678 25. Kakar S, Hoffman FG, Storz JF, Fabian M, Hargrove MS. 2010. Structure and reactivity of
679 hexacoordinate hemoglobins. Biophys Chem 152:1-14.
680 26. Perutz MF. 1990. Mechanisms regulating the reactions of human hemoglobin with oxygen
681 and carbon monoxide. Annu Rev Physiol 52:1-25.
682 27. Ludlow JT, Wilkerson RG, Sahu KK, Nappe TM. 2020. Methemoglobinemia, StatPearls,
683 Treasure Island (FL).
684 28. Balla J, Jacob HS, Balla G, Nath K, Eaton JW, Vercellotti GM. 1993. Endothelial-cell heme
685 uptake from heme proteins: induction of sensitization and desensitization to oxidant
686 damage. Proc Natl Acad Sci U S A 90:9285-9.
687 29. Posta N, Csosz E, Oros M, Petho D, Potor L, Kallo G, Hendrik Z, Sikura KE, Mehes G, Toth C,
688 Posta J, Balla G, Balla J. 2020. Hemoglobin oxidation generates globin-derived peptides in
689 atherosclerotic lesions and intraventricular hemorrhage of the brain, provoking endothelial
690 dysfunction. Lab Invest 100:986-1002.
691 30. Kato GJ, Steinberg MH, Gladwin MT. 2017. Intravascular hemolysis and the pathophysiology
692 of sickle cell disease. J Clin Invest 127:750-760.

693 31. Shaver CM, Upchurch CP, Janz DR, Grove BS, Putz ND, Wickersham NE, Dikalov SI, Ware LB,
694 Bastarache JA. 2016. Cell-free hemoglobin: a novel mediator of acute lung injury. Am J
695 Physiol Lung Cell Mol Physiol 310:L532-41.
696 32. Almeida CB, Souza LE, Leonardo FC, Costa FT, Werneck CC, Covas DT, Costa FF, Conran N.
697 2015. Acute hemolytic vascular inflammatory processes are prevented by nitric oxide
698 replacement or a single dose of hydroxyurea. Blood 126:711-20.
699 33. Rice RH, Lee YM, Brown WD. 1983. Interactions of heme proteins with hydrogen peroxide:
700 protein crosslinking and covalent binding of benzo[a]pyrene and 17 beta-estradiol. Arch
701 Biochem Biophys 221:417-27.
702 34. Nagababu E, Rifkind JM. 1998. Formation of fluorescent heme degradation products during
703 the oxidation of hemoglobin by hydrogen peroxide. Biochem Biophys Res Commun 247:592-
704 6.
705 35. Maitra D, Byun J, Andreana PR, Abdulhamid I, Diamond MP, Saed GM, Pennathur S, Abu-
706 Soud HM. 2011. Reaction of hemoglobin with HOCl: mechanism of heme destruction and
707 free iron release. Free Radic Biol Med 51:374-86.
708 36. Kassa T, Jana S, Strader MB, Meng F, Jia Y, Wilson MT, Alayash AI. 2015. Sickle Cell
709 Hemoglobin in the Ferryl State Promotes betaCys-93 Oxidation and Mitochondrial
710 Dysfunction in Epithelial Lung Cells (E10). J Biol Chem 290:27939-58.
711 37. Nader E, Romana M, Connes P. 2020. The Red Blood Cell-Inflammation Vicious Circle in
712 Sickle Cell Disease. Front Immunol 11:454.
713 38. Buehler PW, Humar R, Schaer DJ. 2020. Haptoglobin Therapeutics and Compartmentalization
714 of Cell-Free Hemoglobin Toxicity. Trends Mol Med 26:683-697.

715 39. Pericone CD, Overweg K, Hermans PW, Weiser JN. 2000. Inhibitory and bactericidal effects of
716 hydrogen peroxide production by Streptococcus pneumoniae on other inhabitants of the
717 upper respiratory tract. Infect Immun 68:3990-7.
718 40. Wu X, Gordon O, Jiang W, Antezana BS, Angulo-Zamudio UA, Del Rio C, Moller A, Brissac T,
719 Tierney ARP, Warncke K, Orihuela CJ, Read TD, Vidal JE. 2019. Interaction between
720 Streptococcus pneumoniae and Staphylococcus aureus Generates (.)OH Radicals That
721 Rapidly Kill Staphylococcus aureus Strains. J Bacteriol 201.
722 41. Lisher JP, Tsui HT, Ramos-Montanez S, Hentchel KL, Martin JE, Trinidad JC, Winkler ME,
723 Giedroc DP. 2017. Biological and Chemical Adaptation to Endogenous Hydrogen Peroxide
724 Production in Streptococcus pneumoniae D39. mSphere 2.
725 42. Taniai H, Iida K, Seki M, Saito M, Shiota S, Nakayama H, Yoshida S. 2008. Concerted action of
726 lactate oxidase and pyruvate oxidase in aerobic growth of Streptococcus pneumoniae: role
727 of lactate as an energy source. J Bacteriol 190:3572-9.
728 43. Pericone CD, Park S, Imlay JA, Weiser JN. 2003. Factors contributing to hydrogen peroxide
729 resistance in Streptococcus pneumoniae include pyruvate oxidase (SpxB) and avoidance of
730 the toxic effects of the fenton reaction. J Bacteriol 185:6815-25.
731 44. Ramos-Montanez S, Kazmierczak KM, Hentchel KL, Winkler ME. 2010. Instability of ackA
732 (acetate kinase) mutations and their effects on acetyl phosphate and ATP amounts in
733 Streptococcus pneumoniae D39. J Bacteriol 192:6390-400.
734 45. Echlin H, Frank M, Rock C, Rosch JW. 2020. Role of the pyruvate metabolic network on
735 carbohydrate metabolism and virulence in Streptococcus pneumoniae. Mol Microbiol
736 doi:10.1111/mmi.14557.

737 46. Echlin H, Frank MW, Iverson A, Chang TC, Johnson MD, Rock CO, Rosch JW. 2016. Pyruvate
738 Oxidase as a Critical Link between Metabolism and Capsule Biosynthesis in Streptococcus
739 pneumoniae. PLoS Pathog 12:e1005951.
740 47. Ramos-Montanez S, Tsui HC, Wayne KJ, Morris JL, Peters LE, Zhang F, Kazmierczak KM, Sham
741 LT, Winkler ME. 2008. Polymorphism and regulation of the spxB (pyruvate oxidase) virulence
742 factor gene by a CBS-HotDog domain protein (SpxR) in serotype 2 Streptococcus
743 pneumoniae. Mol Microbiol 67:729-46.
744 48. Rai P, Parrish M, Tay IJ, Li N, Ackerman S, He F, Kwang J, Chow VT, Engelward BP. 2015.
745 Streptococcus pneumoniae secretes hydrogen peroxide leading to DNA damage and
746 apoptosis in lung cells. Proc Natl Acad Sci U S A 112:E3421-30.
747 49. Brown JL, Yates EA, Bielecki M, Olczak T, Smalley JW. 2018. Potential role for Streptococcus
748 gordonii-derived hydrogen peroxide in heme acquisition by Porphyromonas gingivalis. Mol
749 Oral Microbiol 33:322-335.
750 50. van Beers EJ, Samsel L, Mendelsohn L, Saiyed R, Fertrin KY, Brantner CA, Daniels MP, Nichols
751 J, McCoy JP, Kato GJ. 2014. Imaging flow cytometry for automated detection of hypoxia-
752 induced erythrocyte shape change in sickle cell disease. Am J Hematol 89:598-603.
753 51. Guiral S, Henard V, Laaberki MH, Granadel C, Prudhomme M, Martin B, Claverys JP. 2006.
754 Construction and evaluation of a chromosomal expression platform (CEP) for ectopic,
755 maltose-driven gene expression in Streptococcus pneumoniae. Microbiology (Reading)
756 152:343-349.
757 52. Kjos M, Aprianto R, Fernandes VE, Andrew PW, van Strijp JA, Nijland R, Veening JW. 2015.
758 Bright fluorescent Streptococcus pneumoniae for live-cell imaging of host-pathogen
759 interactions. J Bacteriol 197:807-18.

760 53. Gallay C, Sanselicio S, Anderson ME, Soh YM, Liu X, Stamsas GA, Pelliciari S, van Raaphorst R,
761 Denereaz J, Kjos M, Murray H, Gruber S, Grossman AD, Veening JW. 2021. CcrZ is a
762 pneumococcal spatiotemporal cell cycle regulator that interacts with FtsZ and controls DNA
763 replication by modulating the activity of DnaA. Nat Microbiol 6:1175-1187.
764 54. Mercy C, Ducret A, Slager J, Lavergne JP, Freton C, Nagarajan SN, Garcia PS, Noirot-Gros MF,
765 Dubarry N, Nourikyan J, Veening JW, Grangeasse C. 2019. RocS drives chromosome
766 segregation and nucleoid protection in Streptococcus pneumoniae. Nat Microbiol 4:1661-
767 1670.
768 55. Saito M, Seki M, Iida K, Nakayama H, Yoshida S. 2007. A novel agar medium to detect
769 hydrogen peroxide-producing bacteria based on the prussian blue-forming reaction.
770 Microbiol Immunol 51:889-92.
771 56. Nagababu E, Rifkind JM. 2004. Heme degradation by reactive oxygen species. Antioxid Redox
772 Signal 6:967-78.
773 57. Pamplona A, Ferreira A, Balla J, Jeney V, Balla G, Epiphanio S, Chora A, Rodrigues CD,
774 Gregoire IP, Cunha-Rodrigues M, Portugal S, Soares MP, Mota MM. 2007. Heme oxygenase-1
775 and carbon monoxide suppress the pathogenesis of experimental cerebral malaria. Nat Med
776 13:703-10.
777 58. Mingone CJ, Gupte SA, Chow JL, Ahmad M, Abraham NG, Wolin MS. 2006. Protoporphyrin IX
778 generation from delta-aminolevulinic acid elicits pulmonary artery relaxation and soluble
779 guanylate cyclase activation. Am J Physiol Lung Cell Mol Physiol 291:L337-44.
780 59. Keller LE, Robinson DA, McDaniel LS. 2016. Nonencapsulated Streptococcus pneumoniae:
781 Emergence and Pathogenesis. mBio 7:e01792.

782 60. Facklam R. 2002. What happened to the streptococci: overview of taxonomic and
783 nomenclature changes. Clin Microbiol Rev 15:613-30.
784 61. Kajfasz JK, Rivera-Ramos I, Abranches J, Martinez AR, Rosalen PL, Derr AM, Quivey RG,
785 Lemos JA. 2010. Two Spx proteins modulate stress tolerance, survival, and virulence in
786 Streptococcus mutans. J Bacteriol 192:2546-56.
787 62. van der Hoeven JS, Hoogendoorn H. 1990. Uptake of oxygen, release and degradation of
788 hydrogen peroxide by Streptococcus mutans NCTC 10449. Antonie Van Leeuwenhoek 57:91-
789 5.
790 63. Weiser JN, Ferreira DM, Paton JC. 2018. Streptococcus pneumoniae: transmission,
791 colonization and invasion. Nat Rev Microbiol 16:355-367.
792 64. De Jesus-Bonilla W, Ramirez-Melendez E, Cerda J, Lopez-Garriga J. 2002. Evidence for
793 nonhydrogen bonded compound II in cyclic reaction of hemoglobin I from Lucina pectinata
794 with hydrogen peroxide. Biopolymers 67:178-85.
795 65. Nagababu E, Rifkind JM. 2000. Heme degradation during autoxidation of oxyhemoglobin.
796 Biochem Biophys Res Commun 273:839-45.
797 66. Mao GD, Thomas PD, Poznansky MJ. 1994. Oxidation of spin trap 5,5-dimethyl-1-pyrroline-1-
798 oxide in an electron paramagnetic resonance study of the reaction of methemoglobin with
799 hydrogen peroxide. Free Radic Biol Med 16:493-500.
800 67. Iuliano L, Violi F, Pedersen JZ, Pratico D, Rotilio G, Balsano F. 1992. Free radical-mediated
801 platelet activation by hemoglobin released from red blood cells. Arch Biochem Biophys
802 299:220-4.

803 68. Khan F, Wu X, Matzkin GL, Khan MA, Sakai F, Vidal JE. 2016. Streptococcus pneumoniae
804 Eradicates Preformed Staphylococcus aureus Biofilms through a Mechanism Requiring
805 Physical Contact. Front Cell Infect Microbiol 6:104.
806 69. Regev-Yochay G, Trzcinski K, Thompson CM, Malley R, Lipsitch M. 2006. Interference
807 between Streptococcus pneumoniae and Staphylococcus aureus: In vitro hydrogen peroxide-
808 mediated killing by Streptococcus pneumoniae. J Bacteriol 188:4996-5001.
809 70. Giulivi C, Hochstein P, Davies KJ. 1994. Hydrogen peroxide production by red blood cells.
810 Free Radic Biol Med 16:123-9.
811 71. Assad Z, Michel M, Valtuille Z, Lazzati A, Boizeau P, Madhi F, Gaschignard J, Pham LL, Caseris
812 M, Cohen R, Kaguelidou F, Varon E, Alberti C, Faye A, Angoulvant F, Koehl B, Ouldali N. 2022.
813 Incidence of Acute Chest Syndrome in Children With Sickle Cell Disease Following
814 Implementation of the 13-Valent Pneumococcal Conjugate Vaccine in France. JAMA Netw
815 Open 5:e2225141.
816 72. Akhter F, Womack E, Vidal JE, Le Breton Y, McIver KS, Pawar S, Eichenbaum Z. 2021.
817 Hemoglobin induces early and robust biofilm development in Streptococcus pneumoniae by
818 a pathway that involves comC but not the cognate comDE two-component system. Infect
819 Immun doi:10.1128/IAI.00779-20.
820 73. Akhter F, Womack E, Vidal JE, Le Breton Y, McIver KS, Pawar S, Eichenbaum Z. 2020.
821 Hemoglobin stimulates vigorous growth of Streptococcus pneumoniae and shapes the
822 pathogen's global transcriptome. Sci Rep 10:15202.
823 74. Gotts JE, Bernard O, Chun L, Croze RH, Ross JT, Nesseler N, Wu X, Abbott J, Fang X, Calfee CS,
824 Matthay MA. 2019. Clinically relevant model of pneumococcal pneumonia, ARDS, and
825 nonpulmonary organ dysfunction in mice. Am J Physiol Lung Cell Mol Physiol 317:L717-L736.

826 75. Spellerberg B, Cundell DR, Sandros J, Pearce BJ, Idanpaan-Heikkila I, Rosenow C, Masure HR.
827 1996. Pyruvate oxidase, as a determinant of virulence in Streptococcus pneumoniae. Mol
828 Microbiol 19:803-13.
829 76. Smalley JW, Olczak T. 2017. Heme acquisition mechanisms of Porphyromonas gingivalis -
830 strategies used in a polymicrobial community in a heme-limited host environment. Mol Oral
831 Microbiol 32:1-23.
832 77. O'Brien KL, Bronsdon MA, Dagan R, Yagupsky P, Janco J, Elliott J, Whitney CG, Yang YH,
833 Robinson LG, Schwartz B, Carlone GM. 2001. Evaluation of a medium (STGG) for transport
834 and optimal recovery of Streptococcus pneumoniae from nasopharyngeal secretions
835 collected during field studies. J Clin Microbiol 39:1021-4.
836 78. Livak KJ, Schmittgen TD. 2001. Analysis of relative gene expression data using real-time
837 quantitative PCR and the 2(-Delta Delta C(T)) Method. Methods 25:402-8.
838 79. Vidal JE, Ludewick HP, Kunkel RM, Zahner D, Klugman KP. 2011. The LuxS-dependent
839 quorum-sensing system regulates early biofilm formation by Streptococcus pneumoniae
840 strain D39. Infect Immun 79:4050-60.
841 80. Raimunda D, Padilla-Benavides T, Vogt S, Boutigny S, Tomkinson KN, Finney LA, Arguello JM.
842 2013. Periplasmic response upon disruption of transmembrane Cu transport in
843 Pseudomonas aeruginosa. Metallomics 5:144-51.
844 81. Tavera-Montanez C, Hainer SJ, Cangussu D, Gordon SJV, Xiao Y, Reyes-Gutierrez P, Imbalzano
845 AN, Navea JG, Fazzio TG, Padilla-Benavides T. 2019. The classic metal-sensing transcription
846 factor MTF1 promotes myogenesis in response to copper. FASEB J 33:14556-14574.

847 82. Gordon SJV, Xiao Y, Paskavitz AL, Navarro-Tito N, Navea JG, Padilla-Benavides T. 2019.
848 Atomic Absorbance Spectroscopy to Measure Intracellular Zinc Pools in Mammalian Cells. J
849 Vis Exp doi:10.3791/59519.
850 83. Tettelin H, Nelson KE, Paulsen IT, Eisen JA, Read TD, Peterson S, Heidelberg J, DeBoy RT, Haft
851 DH, Dodson RJ, Durkin AS, Gwinn M, Kolonay JF, Nelson WC, Peterson JD, Umayam LA, White
852 O, Salzberg SL, Lewis MR, Radune D, Holtzapple E, Khouri H, Wolf AM, Utterback TR, Hansen
853 CL, McDonald LA, Feldblyum TV, Angiuoli S, Dickinson T, Hickey EK, Holt IE, Loftus BJ, Yang F,
854 Smith HO, Venter JC, Dougherty BA, Morrison DA, Hollingshead SK, Fraser CM. 2001.
855 Complete genome sequence of a virulent isolate of Streptococcus pneumoniae. Science
856 293:498-506.
857 84. Lanie JA, Ng WL, Kazmierczak KM, Andrzejewski TM, Davidsen TM, Wayne KJ, Tettelin H,
858 Glass JI, Winkler ME. 2007. Genome sequence of Avery's virulent serotype 2 strain D39 of
859 Streptococcus pneumoniae and comparison with that of unencapsulated laboratory strain
860 R6. J Bacteriol 189:38-51.
861 85. Keller LE, Luo X, Thornton JA, Seo KS, Moon BY, Robinson DA, McDaniel LS. 2015.
862 Immunization with Pneumococcal Surface Protein K of Nonencapsulated Streptococcus
863 pneumoniae Provides Protection in a Mouse Model of Colonization. Clin Vaccine Immunol
864 22:1146-53.
865 86. Junges R, Maienschein-Cline M, Morrison DA, Petersen FC. 2019. Complete Genome
866 Sequence of Streptococcus pneumoniae Serotype 19F Strain EF3030. Microbiol Resour
867 Announc 8.

868 87. Keller LE, Thomas JC, Luo X, Nahm MH, McDaniel LS, Robinson DA. 2013. Draft Genome
869 Sequences of Five Multilocus Sequence Types of Nonencapsulated Streptococcus
870 pneumoniae. Genome Announc 1.
871 88. Boake WC. 1956. Antistaphylocoagulase in experimental staphylococcal infections. J
872 Immunol 76:89-96.

873
874
875
876
877
878
879
880
881
882
883
884
885
886
887

888 **Table 1. Quantification of cell-free hemoglobin and the heme-hemoglobin Soret curve.**

| **Strains** | **Cell-free hemoglobin (μM)** | **Absorbance at 415 nm** |
|---|---|---|
| Uninfected | 17.35 | 1.38 |
| TIGR4 | 12.8 | 1.39 |
| TIGR4Δ*spxB*Δ*lctO* | 16.4 | 1.21 |

889

890

891

**Table 2. Strains utilized in this study.**

| Strain | Characteristics | Reference or source |
|---|---|---|
| TIGR4 | Reference strain, whole genome sequenced, capsular serotype 4 | (83) |
| SPJV41 (TIGR4Δ*spxB*Δ*lctO*) | TIGR4 with a deleted *spxB* and *lctO* gene by insertion-deletion with an erythromycin and spectinomycin cassette, respectively | (40) |
| SPJV29 (TIGR4Δ*spxB*) | TIGR4 with an insertionally inactivated *spxB*::*ermB* (Ery$^r$) | (23) |
| SPJV42 (TIGR4Δ*lctO*) | TIGR4 with an insertionally inactivated *lctO*:: *aad9* (Spc$^r$) | (40) |
| SPJV43 (TIGR4Δ*spxB*Ω*spxB*) | SPJV29 complemented with the gene *spxB* and its promoter | This study |
| SPJV44 (TIGR4Δ*spxB*Δ*lctO*Ω*spxB*- | SPJV41 complemented with the gene | This study |

| | | |
|---|---|---|
| *lctO*) | *spxB* and *lctO* | 907 |
| D39 | Avery strain, clinical isolate, capsular serotype 2 | (84) 908 |
| P878 | D39 with a deletion in *spxB* | (39) 909 |
| P1221 | P878 complemented with pMU1328::*spxB* | (43) 910 |
| SPJV45 (D39Δ*spxB*Δ*lctO*) | D39 with a deleted *spxB* and *lctO* gene by insertion-deletion with an erythromycin and spectinomycin cassette, respectively | (23) 911 912 |
| EF3030 | Clinical isolate, caccine serotype 19F strain | (85, 86) 913 |
| SPJV49 (EF3030Δ*spxB*Δ*lctO*) | EF3030 with a deleted *spxB* and *lctO* gene by insertion-deletion with an erythromycin and spectinomycin cassette, respectively | (23) 914 915 |
| SPJV50 (EF3030Δ*spxB*) | EF3030 with an insertionally inactivated *spxB*::*ermB* (Ery$^r$) | This study 916 |
| SPJV51 (EF3030Δ*lctO*) | EF3030 with an insertionally inactivated *lctO*:: *aad9* (Spc$^r$) | This study 917 |
| MNZ41 | Non-encapsulated *S. pneumoniae* strain | (87) 918 |
| MNZ67 | Non-encapsulated *S. pneumoniae* strain | (87) |
| *S. pseudopneumoniae* | ATCC 960 | Laboratory stock 919 |
| *S. salivarius* | ATCC 7073 | Laboratory stock 920 |
| *S. oralis* | ATCC 35037 | Laboratory stock 921 |
| *K. pneumoniae* | ATCC 700603 | Laboratory stock 922 |
| *Staphylococcus aureus* strain Newman | NCTC 8178, ATCC 13420 | (88) 923 |
| Non-typeable *Haemophilus influenzae* (NTHI) | M5029 | Laboratory stock 924 |
| *S. mitis* | ATCC 49456 | Laboratory stock 925 |
| *S. mutans* | ATCC 25175 | Laboratory stock 926 |

**Table 3. Oligonucleotides designed and used in this study** 927

| Primer | Sequence (5→ 3) |
|---|---|
| hlpA-up1 | TCAGCAGGTTCATGAGGGAA |

| | |
|---|---|
| hlpA-up2 | TCATTTCTGTTTTATAACAAAGTCCGGATCCTTTAACAGCGT |
| hlpA-down1 | CTCGCCGAAAATCAAATATGATCACTCACGGCATGGATGA |
| hlpA-down2 | CAAAACAACATTGCCCGACG |
| spxB1 | CTTTGTTATAAAACAGAAATGA |
| spxB2 | CATATTTGATTTTCGGCGAG |
| hlpA-up3 | TTTCCCCAATTATTCACCCCACATATTTGATTTTCGGCGAG |
| lcto1 | TGGGGTGAATAATTGGGGAAA |
| lcto2 | CATTCAGTGGAGGCAATCTGT |
| lcto-spec1 | TTTCTGAGTAGGCGGAGTGG |
| lcto-spec2 | GCAATTTTCAGAGCAGCTTGG |
| JVS109L | TCTACTCAATCGACGTAGGTAACA |
| JVS110R | TATTGAACGTTTGTGATAACGTCT |
| JVS59L | TGAGACTAAGGTTACAGCTTACAG |
| JVS60R | CTAATTTTGACAGAGAGATTACGA |
| JVS105L | TTTGCAATGTAGAAAATCCAAGTA |
| JVS106R | AAATCTCTGGAAGGTCAACAGTAG |
| JVS49L | CTGATGACTGTCAATCGAGATACC |
| JVS50R | AATGGACGAATCAACTCCATAA |
| JVS35L | AACCAAGTAACTTTGAAAGAAGAC |
| JVS36R | AAATTTAGAATCGTGGAATTTTT |

928

929

930

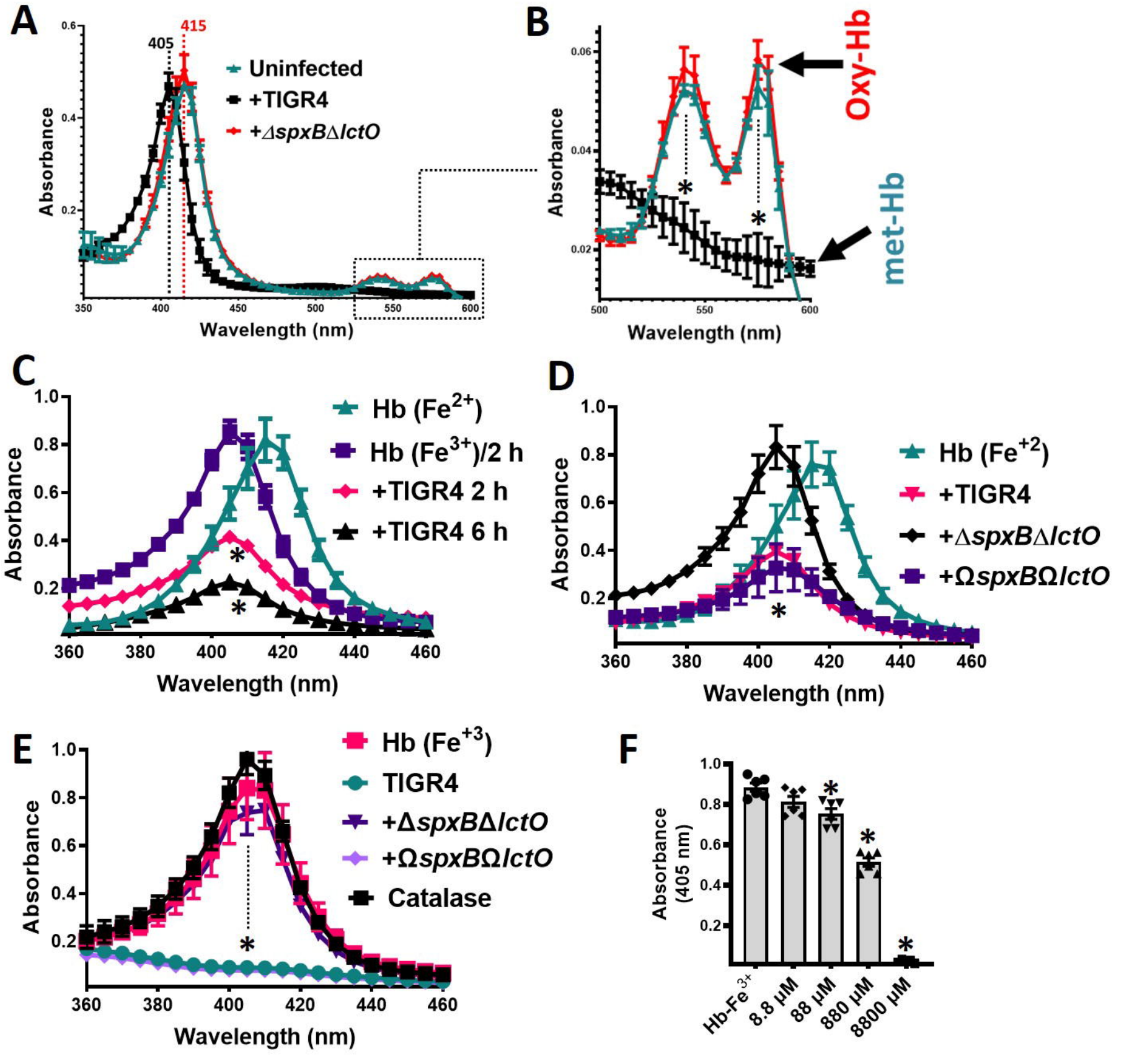
A
415
405
Uninfected
+TIGR4
+ΔspxBΔlctO
Absorbance
Wavelength (nm)
B
Oxy-Hb
met-Hb
Absorbance
Wavelength (nm)
C
Hb (Fe2+)
Hb (Fe3+)/2 h
+TIGR4 2 h
+TIGR4 6 h
Absorbance
Wavelength (nm)
D
Hb (Fe+2)
+TIGR4
+ΔspxBΔlctO
+ΩspxBΩlctO
Absorbance
Wavelength (nm)
E
Hb (Fe+3)
TIGR4
+ΔspxBΔlctO
+ΩspxBΩlctO
Catalase
Absorbance
Wavelength (nm)
F
Absorbance (405 nm)
Hb-Fe3+
8.8 μM
88 μM
880 μM
8800 μM

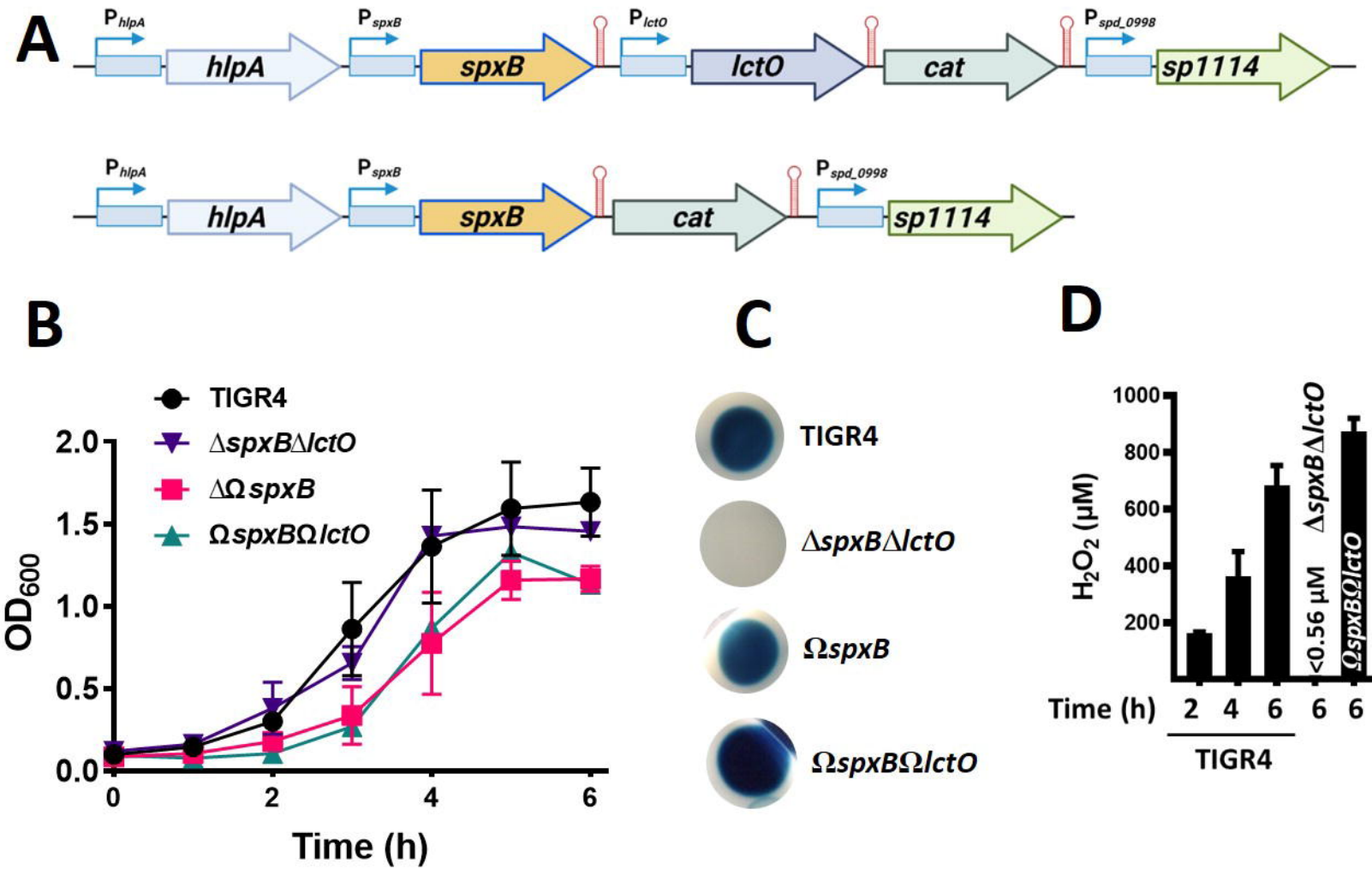
A
P hlpA
hlpA
P spxB
spxB
P lctO
lctO
cat
P spd_0998
sp1114
B
TIGR4
ΔspxBΔlctO
ΔΩspxB
ΩspxBΩlctO
OD600
Time (h)
C
TIGR4
ΔspxBΔlctO
ΩspxB
ΩspxBΩlctO
D
H2O2 (μM)
<0.56 μM
ΔspxBΔlctO
ΩspxBΩlctO
Time (h)
TIGR4

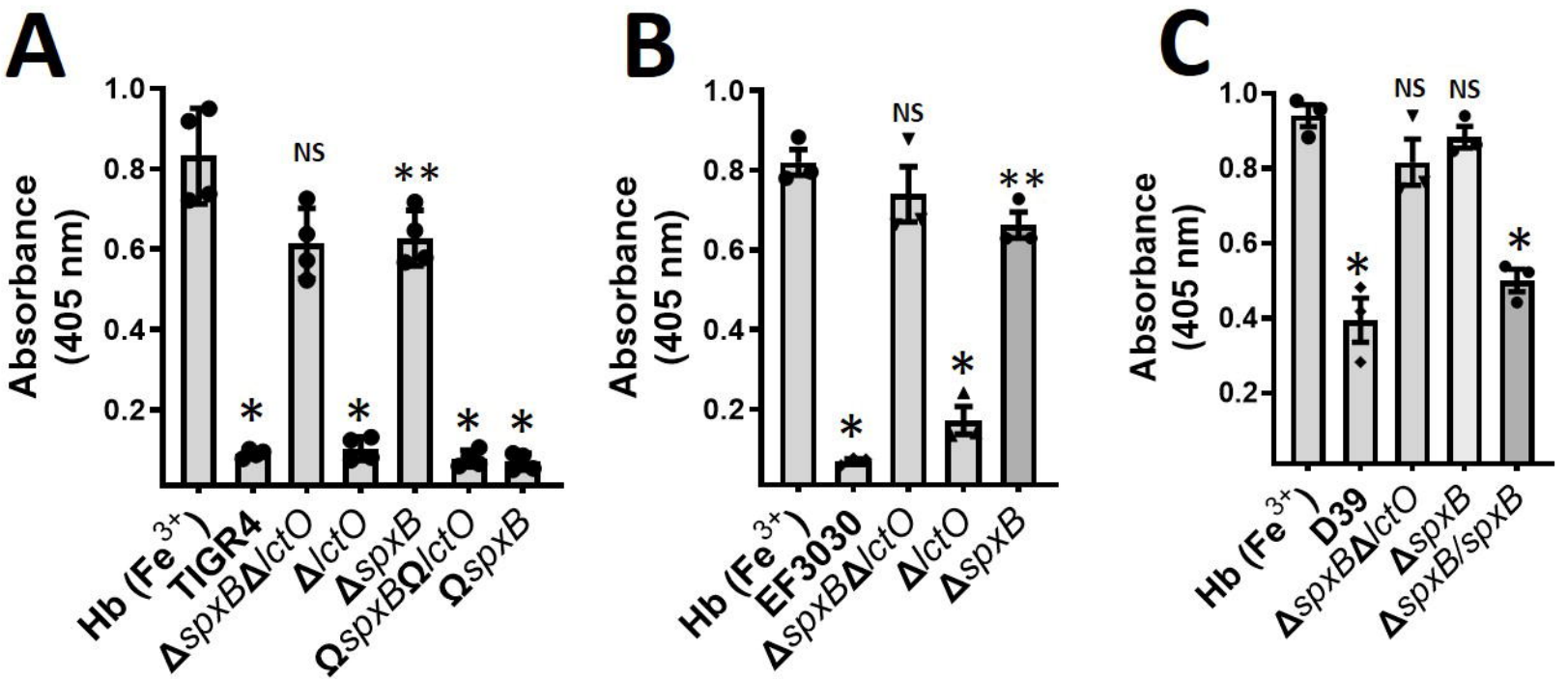
A
B
C
Absorbance (405 nm)
1.0
0.8
0.6
0.4
0.2
NS
*
**
Hb (Fe3+)
TIGR4
ΔspxBΔlctO
ΔlctO
ΔspxB
ΩspxBΩlctO
ΩspxB
EF3030
D39
ΔspxB/spxB

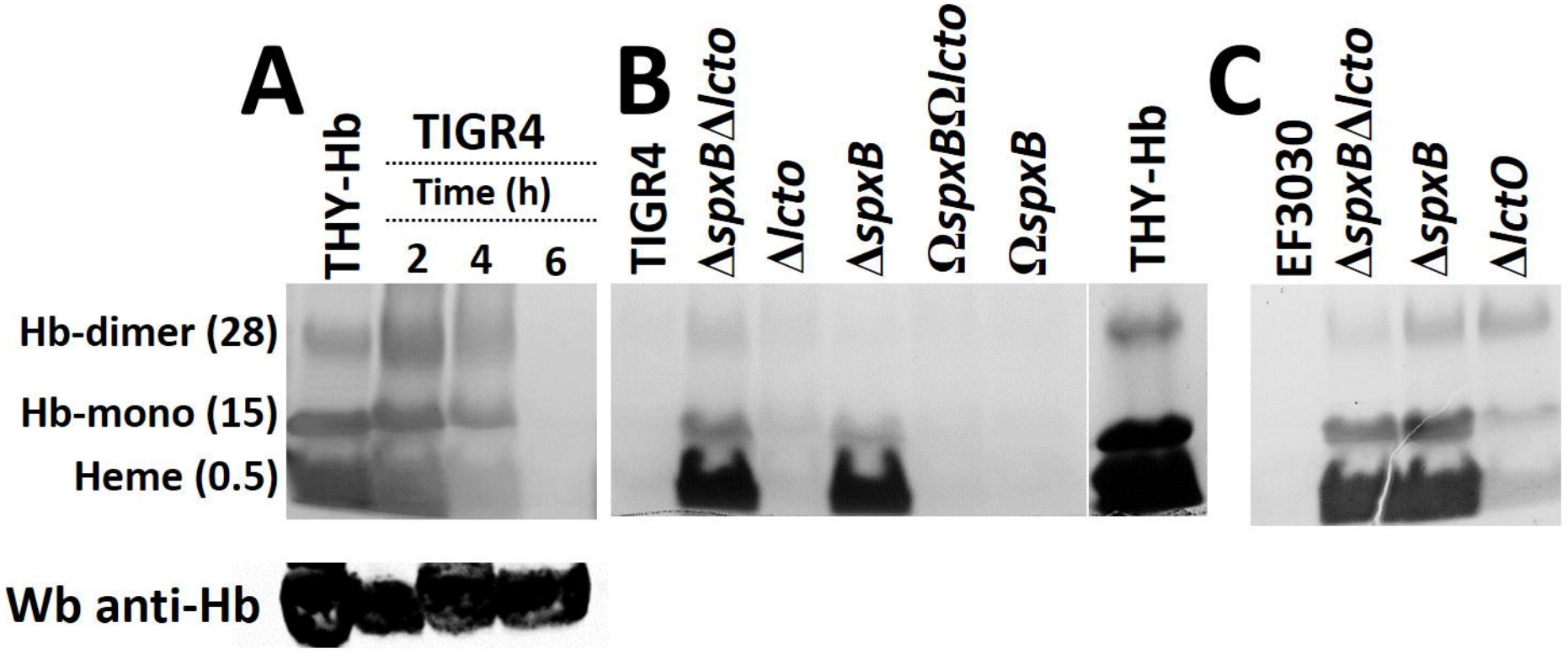
A
THY-Hb
TIGR4
Time (h)
2
4
6
Hb-dimer (28)
Hb-mono (15)
Heme (0.5)
Wb anti-Hb
B
TIGR4
ΔspxBΔlcto
Δlcto
ΔspxB
ΩspxBΩlcto
ΩspxB
THY-Hb
C
EF3030
ΔspxBΔlcto
ΔspxB
ΔlctO

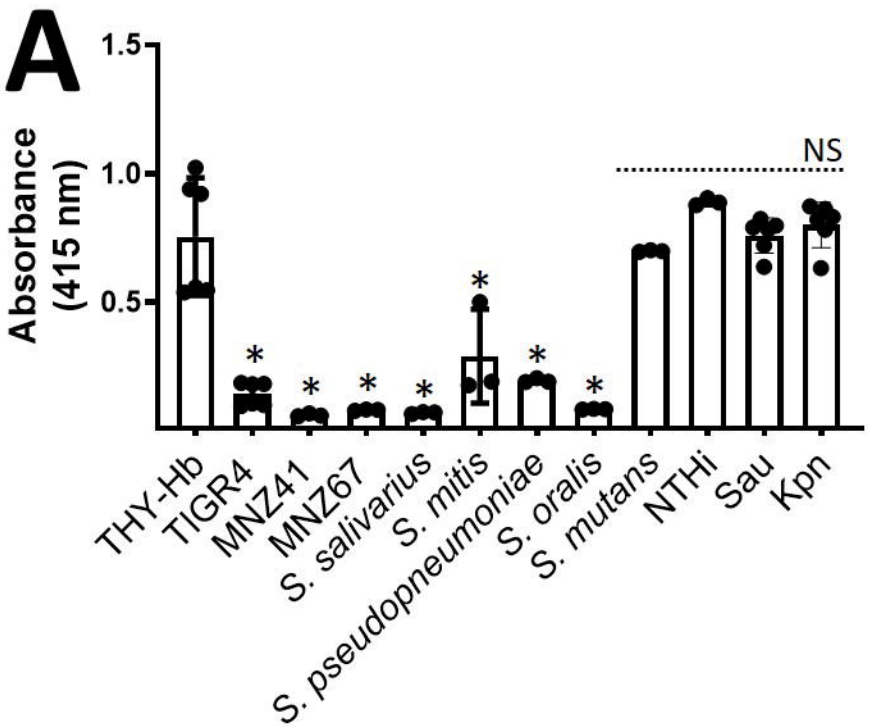
A
Absorbance (415 nm)
1.5
1.0
0.5
NS
*
THY-Hb
TIGR4
MNZ41
MNZ67
S. salivarius
S. mitis
S. pseudopneumoniae
S. oralis
S. mutans
NTHi
Sau
Kpn

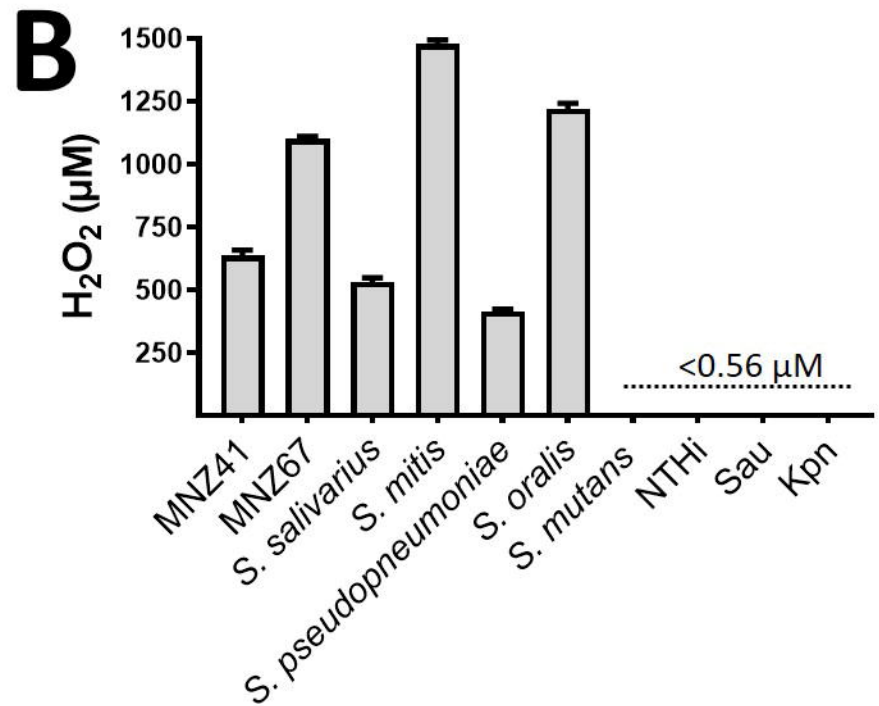
B
$H_2O_2$ (μM)
1500
1250
1000
750
500
250
<0.56 μM
MNZ41
MNZ67
S. salivarius
S. mitis
S. pseudopneumoniae
S. oralis
S. mutans
NTHi
Sau
Kpn

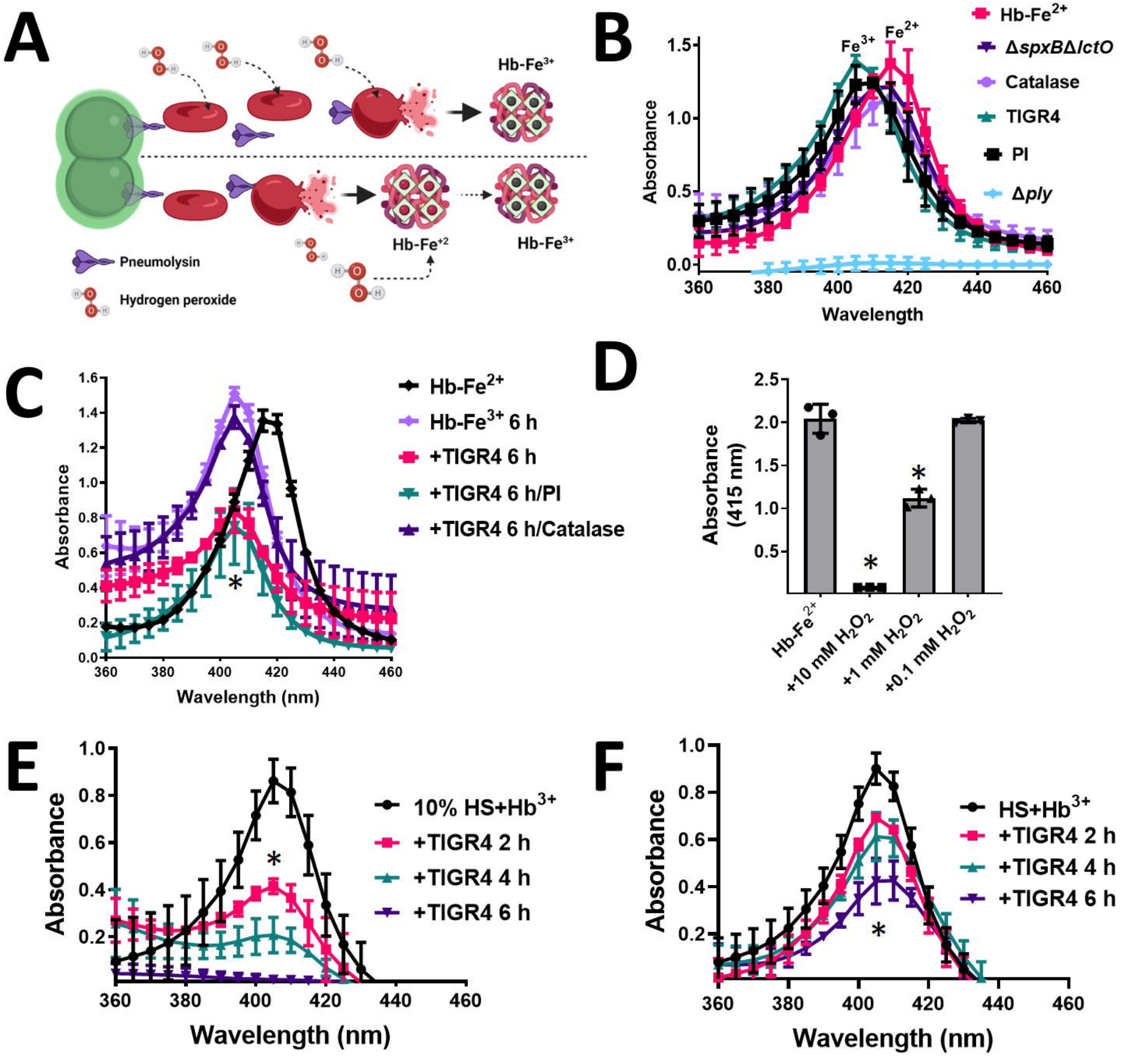
A
Hb-Fe3+
Hb-Fe+2
Hb-Fe3+
Pneumolysin
Hydrogen peroxide
B
Hb-Fe2+
ΔspxBΔlctO
Catalase
TIGR4
PI
Δply
Fe3+
Fe2+
Absorbance
Wavelength
C
Hb-Fe2+
Hb-Fe3+ 6 h
+TIGR4 6 h
+TIGR4 6 h/PI
+TIGR4 6 h/Catalase
Absorbance
Wavelength (nm)
D
Absorbance (415 nm)
Hb-Fe2+
+10 mM H2O2
+1 mM H2O2
+0.1 mM H2O2
E
10% HS+Hb3+
+TIGR4 2 h
+TIGR4 4 h
+TIGR4 6 h
Absorbance
Wavelength (nm)
F
HS+Hb3+
+TIGR4 2 h
+TIGR4 4 h
+TIGR4 6 h
Absorbance
Wavelength (nm)

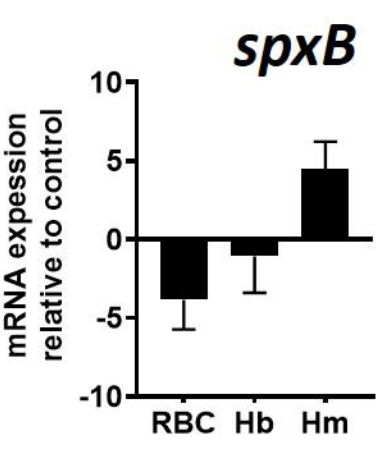
spxB
mRNA expression relative to control
10
5
0
-5
-10
RBC
Hb
Hm

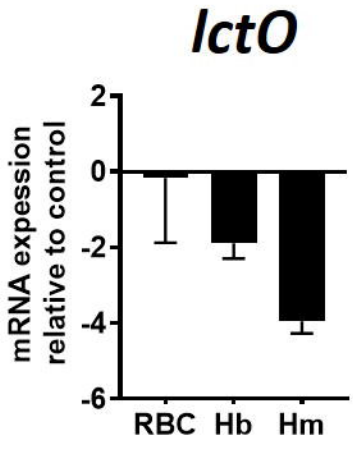
lctO
mRNA expression relative to control
2
0
-2
-4
-6
RBC
Hb
Hm

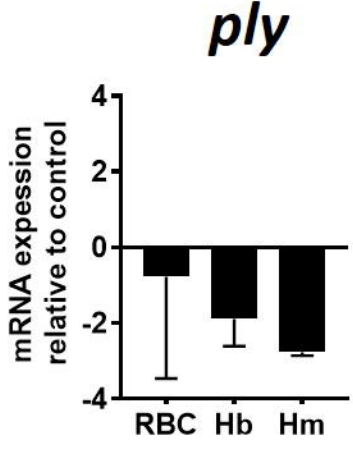
ply
mRNA expression relative to control
4
2
0
-2
-4
RBC
Hb
Hm